

People's Democratic Republic of Algeria  
Ministry of Higher Education and Scientific Research  
National Polytechnic School



Department of Metallurgy  
End-of-Study Project Thesis  
Submitted in Fulfillment of the Requirements for the Degree of

**State Engineer in Materials Engineering**

Entitled:

# Application of Design of Experiments in Gas Nitriding of Steels

by

■ Mr. Omar KHELIFA

Under the Supervision of

■ Mr. M. E. DJEGHLAL Professor

■ Mr. L. BENALIA PhD Student

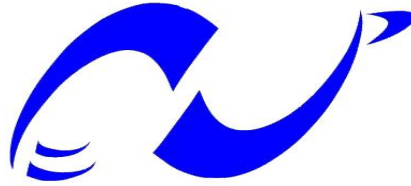
Submitted for Defense on 02 July 2020

Members of Jury

■	<b>President</b>	Mr. K. ABADLI	MAA	ENP
■	<b>Supervisor</b>	Mr. M. E. DJEGHLAL	Professor	ENP
■	<b>Examiners</b>	Mr. A. BOUDIAF Mr. L. HEMMOUCHE	MCA MCB	EMP EMP



People's Democratic Republic of Algeria  
Ministry of Higher Education and Scientific Research  
National Polytechnic School



المدرسة الوطنية المتعددة التقنيات  
Ecole Nationale Polytechnique

Department of Metallurgy  
End-of-Study Project Thesis  
Submitted in Fulfillment of the Requirements for the Degree of

## State Engineer in Materials Engineering

Entitled:

# Application of Design of Experiments in Gas Nitriding of Steels

by

■ Mr. Omar KHELIFA

Under the Supervision of

■ Mr. M. E. DJEGHLAL                      Professor  
■ Mr. L. BENALIA                              PhD Student

Submitted for Defense on 02 July 2020

Members of Jury

■	<b>President</b>	Mr. K. ABADLI	MAA	ENP
■	<b>Supervisor</b>	Mr. M. E. DJEGHLAL	Professor	ENP
■	<b>Examiners</b>	Mr. A. BOUDIAF Mr. L. HEMMOUCHE	MCA MCB	EMP EMP

---

## Acknowledgment

First and foremost, all the praises and thanks be to **ALLAH**, the Lord of the Worlds, and Prayers of **ALLAH** are to Muḥammad and his Family and Companions until the Day of Resurrection.

This having been said, I hereby express my deepest gratitude to my father, my mother, and all of my family members for their constant support and understanding, from my first day of study, until the presentation of this project.

My sincerest appreciation is to my supervisors, Pr. DJEGHLAL, for his expert instructions, advices, mentoring, and motivation, and Mr. BENALIA, for his guidance and pertinent remarks. Without their great knowledge, I would not have been able to overcome all the obstacles that I encountered during this journey of my End-of-Study project.

I would like to present my thankfulness to the President of the Jury, Dr. ABADLI, and the other members: Mr. BOUDIAF and Mr. HEMMOUCHE from Ecole Militaire Polytechnique, for accepting to be part of the dissertation committee and generously offering their time to review this manuscript and present constructive analysis on the present work.

I also wish to sincerely thank all those who provided assistance and encouragement, from near and far, for the sake of completing this thesis.

Last but not least, I would like to take this opportunity to convey my profound recognition for my teachers at the Metallurgy department at the National Polytechnic School, especially the Head of Department, Pr. CHITROUB, for the knowledge they have provided, for the patience they have observed, and for having been more like a fatherly figure for me throughout my years as a student in the department.

At last, as at first, in all circumstances, and always, all the praises and thanks be to **ALLAH**, the Lord of the Worlds.

---

## ملخص

يُدرُسُ هذا العمل تطبيق طريقة تخطيط التجارب على النتردة الغازية للفولاذ، وهي معالجة كيميائية حرارية للسطوح. وتكمن قيمة هذا البحث في نمذجة النتردة الغازية للفولاذ بُغية مقارنة تأثيرات العوامل التجريبية على سُمك الطبقة المُنتردة، وتحسينه عند قيمة مُراداة، دون الحاجة إلى أعمال تجريبية شاقة ومُكلفة. إذ بتطبيق تقنية الانحدار الخطي على بيانات تجريبية لنتردة غازية للفولاذ 35CrMo12 صُنِعَ مخطط عوامل كامل بثلاثة متغيرات لكل منها ثلاثة مستويات. ثم تُحَقَّقُ من صحة هذا النموذج بالتحليل الإحصائي. وبَيَّنَتِ النَّتَائِجُ أن لدرجة حرارة النتردة التأثير الأكبر على سُمك الطبقة المُنتردة، يليها كُمون النتردة ثم زمنها. ويُعَدُّ الجانب الواعد في استعمال تخطيط التجارب هو بلوغ معادلة رياضية تعطي سُمك الطبقة المُنتردة بدلالة درجة الحرارة والزمن والكُمون، إذ سيسمح هذا بتيسير الأعمال التجريبية وتحسينها. ومن المتوقع أن يفتح هذا العمل الباب لبحوث أخرى في مجال نمذجة النتردة الغازية للفولاذ باستعمال طريقة تخطيط التجارب.

**الكلمات الدالة:** النتردة الغازية، تخطيط التجارب، سُمك الطبقة المُنتردة، درجة حرارة النتردة، زمن النتردة، كُمون النتردة، التحسين، الفولاذ 35CrMo12.

## Résumé

Ce travail étudie l'application de la méthodologie des Plans d'Expériences (DoE) dans le traitement thermo-chimique de surface des aciers par Nitruration Gazeuse. La principale contribution réside dans la modélisation de la Nitruration Gazeuse des aciers afin de comparer les effets de facteurs sur la Profondeur de la Couche Nitrurée et d'optimiser cette dernière pour une certaine valeur, sans avoir à réaliser des procédures expérimentales coûteuses et exhaustives. En appliquant la technique de Régression Linéaire sur des données expérimentales de Nitruration Gazeuse de l'acier 35CrMo12, un plan factoriel complet de trois facteurs à trois niveaux a été créé. Le modèle a ensuite été validé avec succès par des analyses statistiques. Les résultats ont révélé que la température de nitruration a la plus grande influence sur la Profondeur de la Couche Nitrurée, suivie par le potentiel, puis le temps. La partie prometteuse de l'utilisation des Plans d'Expériences est l'établissement d'une équation mathématique de la Profondeur de la Couche Nitrurée en fonction de la température, temps et potentiel, car cela permettrait d'optimiser et de faciliter les procédures expérimentales. Il est prévu que ce travail serait le principal moteur de plusieurs projets de recherche sur la modélisation de la Nitruration Gazeuse en utilisant les Plans d'Expériences.

**Mots-clés :** Nitruration Gazeuse, Plans d'Expériences, Profondeur de la Couche Nitrurée, Température de Nitruration, Temps de Nitruration, Potentiel de Nitruration, Optimisation, Acier 35CrMo12.

---

## **Abstract**

This work deals with the application of Design of Experiments (DoE) method in Gas Nitriding surface thermochemical treatment of steels. The main contribution herein lies in modeling the Gas Nitriding of steels in order to compare factors effects on the Nitrided Layer (NL) depth as well as optimizing this latter for a certain value, without having to perform expensive and exhaustive experimental procedures. By applying the technique of Linear Regression on Gas Nitriding experimental data of the steel 35CrMo12, a full factorial design of three factors with three levels was created. The model was then successfully validated through statistical analysis. The results revealed that the nitriding temperature has the greatest influence on the NL depth, followed by potential, and then time. The promising part of employing Design of Experiments is establishing a mathematical equation of NL depth as function of temperature, time and potential, as this would optimize and facilitate experimental procedures. It is envisaged that this work would be the main driver for several research projects in Gas Nitriding modeling utilizing Design of Experiments.

**Keywords:** Gas Nitriding, Design of Experiments, Nitrided Layer Depth, Nitriding Temperature, Nitriding Time, Nitriding Potential, Optimization, 35CrMo12 Steel.

---

---

# Table of Contents

## Table of Contents

### List of Tables

### List of Figures

### General Conclusion

I.	Chapter One: Bibliographic Study on the Diffusion Phenomenon.....	15
I.1	Introduction .....	15
I.2	Definition.....	15
I.3	Types of Diffusion .....	16
I.4	Diffusion Mechanisms .....	16
I.5	Diffusion and Temperature.....	19
I.6	Fundamental Laws of Diffusion.....	19
I.6.1	Diffusion Equation in Three Dimensions .....	20
I.6.2	Solutions of the Diffusion Equation.....	21
I.7	Conclusion.....	22
II.	Chapter Two: Bibliographic Study on Nitriding.....	24
II.1	Introduction .....	24
II.2	Principle.....	24
II.3	Nitriding Steels .....	24
II.4	Phase Diagrams .....	25
II.4.1	Binary Diagram Fe-N .....	25
II.4.2	Ternary Diagram Fe-N-C .....	27
II.4.3	Complex Diagram Fe-N-C-X.....	28
II.5	Structures of The Formed Layers .....	29
II.5.1	The Compound Layer.....	31
II.5.2	The Nitride $Fe_4N_{2-3}$ .....	32
II.5.3	The Nitride $Fe_4N_{2-3}$ .....	32
II.5.4	The Diffusion Layer .....	32
II.6	Enthalpy of Formation .....	33
II.7	Influence of Alloying Elements.....	34
II.7.1	Influence of Aluminium .....	36
II.7.2	Influence of Chromium.....	36
II.7.3	Influence of Molybdenum .....	36
II.7.4	Influence of Nickel .....	37
II.7.5	Influence of Vanadium .....	37

---

---

II.8	Nitriding Types .....	37
II.9	Gas Nitriding .....	38
II.9.1	Gas Nitriding Fundamental Factors .....	40
II.10	Conclusion .....	43
III.	Chapter Three: Bibliographic Study on Design of Experiments.....	45
III.1	Introduction .....	45
III.2	Experimental Design Objectives .....	46
III.2.1	DoE Advantages .....	47
III.3	Implementing a Design of Experiments .....	47
III.4	Defining Research Problem.....	48
III.4.1	Factors .....	49
III.4.2	Experimental Domain.....	50
III.4.3	Response.....	50
III.5	Linear Regression Analysis .....	51
III.6	Full and Fractional Factorial Experiments.....	51
III.6.1	Full Factorial Designs .....	52
III.6.2	Fractional Factorial Designs.....	52
III.6.3	Experimental Matrix .....	52
III.7	Conclusion.....	54
IV.	Chapter Four: Modeling of Gas Nitriding of a Steel by Design of Experiments .....	56
IV.1	Introduction .....	56
IV.2	Investigated Steel .....	56
IV.3	Defining Research Problem .....	58
IV.3.1	Responses.....	58
IV.3.2	Factors .....	58
IV.3.3	Experimental Domain.....	59
IV.4	Mathematical Model .....	60
IV.5	Factorial Designs.....	61
IV.5.1	Full Factorial Design .....	61
IV.5.2	Fractional Factorial Design.....	66
IV.5.3	Comparing the two Models.....	70
IV.6	Statistical Analysis.....	71
IV.7	Study of Factors Effects on the Nitrided Layer Depth.....	74
IV.8	Testing the Model Using Experimental Examples .....	76
IV.9	Graphical Representation of NL Depth Function .....	76
IV.10	Conclusion .....	80

---



---

V. Chapter Five: Optimizing a Response Using the DoE Model.....	82
V.1 Introduction .....	82
V.2 Definition.....	82
V.3 Optimizing the Nitrided Layer Depth.....	82
V.3.1 Optimization Algorithm .....	83
V.3.2 Results and Discussion.....	84
V.4 Validating the Algorithm.....	86
V.5 Conclusion.....	87
General Conclusion .....	89
References.....	92

---

---

## List of Tables

Table II-1. List of nitrides that may be formed from addition elements.....	34
Table II-2. Comparison between the different types of nitriding.....	38
Table III-1. Experimental matrix.....	53
Table IV-1. Chemical composition (in wt %) of the steel investigated.....	56
Table IV-2. Factors levels .....	58
Table IV-3 Experimental matrix for the 3 <sup>3</sup> full factorial design relevant to gas nitriding of the steel 35CrMo12.....	63
Table IV-4. Coefficients of the 3 <sup>3</sup> full factorial model relevant to gas nitriding of the steel 35CrMo12.....	64
Table IV-5. Comparison between the experimental NL depths and the ones predicted by the full factorial model .....	65
Table IV-6. Taguchi combinations for the fractional factorial 3 <sup>3</sup> design .....	67
Table IV-7. Experimental matrix for the Taguchi 3 <sup>3</sup> fractional factorial design relevant to gas nitriding of the steel 35CrMo12 .....	68
Table IV-8. Coefficients of the Taguchi 3 <sup>3</sup> fractional factorial model relevant to gas nitriding of the steel 35CrMo12.....	68
Table IV-9. Comparison between the experimental NL depths and the ones predicted by the fractional factorial model .....	69
Table IV-10. Results of linear regression analysis.....	72
Table IV-11. Statistical test results for the full factorial model coefficients.....	74
Table IV-12. Minimum and maximum values of NL depth function.....	78

---

---

## List of Figures

Figure I.1. Auto-diffusion in the same material .....	16
Figure I.2. Pre and post-diffusion concentration profiles.....	16
Figure I.3. Direct interstitial mechanism of diffusion.....	17
Figure I.4. A simulated motion of atoms chain in an amorphous Ni-Zr alloy.....	17
Figure I.5. Monovacancy mechanism of diffusion.....	18
Figure I.6. Divacancy mechanism of diffusion.....	18
Figure I.7. Interstitialcy mechanism of diffusion .....	18
Figure I.8. Interstitial-substitutional exchange mechanisms of foreign atom diffusion...	19
Figure I.9. Illustration of Fick's first law.....	20
Figure I.10. Cartesian coordinates .....	21
Figure I.11. Boundary and initial conditions of the diffusion equation.....	21
Figure I.12. Concentration profile according to different diffusion times .....	22
Figure II.1. Iron-nitrogen equilibrium diagram.....	26
Figure II.2. Structure of the nitride $\gamma'$ .....	26
Figure II.3. Nitride structure $\text{Fe}_2\text{N}-\text{Fe}_3\text{N}$ .....	27
Figure II.4. Isothermal cut at 580°C of the Fe-N-C equilibrium diagram.....	28
Figure II.5. Nitrogen and carbon concentrations as function of depth of a nitrided steel	29
Figure II.6. Effect of nitrogen and carbon profiles on the microstructure of a nitrided steel .....	29
Figure II.7. Microstructure of the nitrided zone of a steel.....	30
Figure II.8. Micrograph of the nitrided layer of steel 32CrMoV13. Nital attack 3%.....	30
Figure II.9. M.E.B. micrograph of the nitrided layer of the steel 32CrMoV13.....	31
Figure II.10. Nitride case profiles for various steels .....	33
Figure II.11. Effect of alloying elements on the activity coefficient of nitrogen in iron at 500 °C .....	35
Figure II.12. Mode of interaction between alloying elements and nitrogen .....	36
Figure II.13. Tempering furnace .....	39
Figure II.14. Gas nitriding furnace .....	40
Figure II.15. Pressurized gas nitriding scheme.....	42
Figure III.1. The circular flow of scientific learning .....	46
Figure III.2. Experimental Domain .....	50
Figure IV.1. TTT diagram for 35CrMo12, simulated with JMatPro .....	57
Figure IV.2. CTT diagram for 35CrMo12, simulated with JMatPro .....	57
Figure IV.3. Experimental domain .....	60
Figure IV.4. Comparing the full factorial model to experimental data .....	66
Figure IV.5. Comparing the fractional factorial model to experimental data .....	69
Figure IV.6. Effects of factors on the NL depth in case of full factorial design.....	75
Figure IV.7. Effects of factors on the NL depth in case of fractional factorial design.....	75
Figure IV.8. NL depth plot at fixed values of potential.....	77
Figure IV.9. NL depth plot at fixed values of time .....	77
Figure IV.10. NL depth plot at fixed values of temperature.....	78
Figure IV.11. NL depth as function of time .....	79
Figure V.1. Output for NL depth of 600 $\mu\text{m}$ .....	85
Figure V.2 Output in case of NL depth of 655.75 $\mu\text{m}$ .....	87
Figure V.3 Output in case of NL depth of 533.17 $\mu\text{m}$ .....	87

---

---

# **General Introduction**

---

## General Introduction

Throughout the history of mankind, developing materials has been among the greatest achievements of every age, as it has symbolized the growth, prosperity, quality and security of human beings.

Materials Engineering is the science of improving and developing materials in order to fulfill a certain need. Hence, it covers almost all aspects of life.

Materials engineers are at the forefront of many areas of science, as they manipulate the properties of matters to open the door to new technologies. The properties of a given material are intimately related to its structure, at all levels: how the atoms are joined, and how groups of atoms are arranged throughout the material. A material may be chosen for a certain function for several criteria, namely its hardness, electrical properties, resistance to heat or corrosion, and many other qualities.

The job of a materials engineer is complicated as it does not only require knowledge of several scientific fields, namely physics, chemistry, electricity, and of course, mathematics, but also to take into consideration the economic, social and environmental aspects.

Among the techniques used in Materials Engineering to improve the performance of materials there is surface treatment, which is a process applied on the surface of a material in order to improve its mechanical properties, namely hardness, corrosion resistance, leisure resistance, wear resistance, etc.

Historically, thermochemical treatments were limited to mechanical parts that are machined, forged or laminated with applications in industrial machinery, automotive industry, tooling, oil drilling, mining and defense<sup>[1]</sup>. Practically, steel was the only material subject to change. The key process consisted in nitriding, carburizing (case-hardening) and their combinations. The modifications of the thermochemical treatments included other processes such as boriding, aluminizing, chromizing or other diffusions thermo-reactive materials exploring vanadium, molybdenum and other elements.

Hence, surface engineering represents an attractive and economically viable method to improve the surface layer of materials. Since this latter conditions its lifespan in several applications. Its objective is to develop a wide range of different functional properties of the substrate including physical, chemical, electrical, electronic, magnetic or mechanical properties. Part of surface engineering, thermochemical treatments use thermal diffusion for incorporating metallic or non-metallic atoms into the surface of a material to modify its chemical composition and its microstructure<sup>[2]</sup>.

Nitriding is a surface treatment in which nitrogen (N) diffuses into a material for the sake of improving its mechanical properties. One of the most used nitriding techniques is gas nitriding, which consists of providing the surface of the material with Ammonia gas. This method has several advantages, namely the simplicity of its equipment, low cost, and the ability to treat large parts, not to mention its technical advantages by means of improving the mechanical and chemical properties.

Conventionally, the experimenter's work consists of constantly varying the parameters of the phenomenon in question in order to determine which are responsible of greater changes in the system as well as their impact on the final result. Yet this method is time consuming, involves considerable effort, and even inaccurate. Hence, researchers are recently giving further attention to optimization and simulation methods, in order to acquire acceptable results with the least time and effort possible.

Design of Experiments is a statistical optimization method that aims to acquire more precise data and more complete information on a studied phenomenon with a minimal number of experiments and the lowest possible material costs<sup>[19]</sup>. Thus, it aims to facilitate the experimental as well as the simulation work for researchers. Furthermore, it establishes the conditions under which the parameters should work in order to optimize the process<sup>[15]</sup>.

Although several attempts have been made in the literature to model and simulate the gas nitriding of steels, no research work has yet employed the Design of Experiments method.

Within the framework of this graduation project, the objective is to study the application of Design of Experiments in gas nitriding of steels. Thereby evaluating the advantages and results of using this method. The main purposes are investigating the influence of each of

gas nitriding parameters: temperature, time and potential, on the nitrided layer depth, along with using the established model for optimizing the depth at a certain desired value.

The remainder of this manuscript is organized as follows:

The first three chapters contain bibliographic studies. Chapter one briefly presents the diffusion phenomenon. Chapter two, introduces the nitriding surface treatment, including gas nitriding, while chapter three is dedicated to Design of Experiments.

Then, the performed work and the results of modeling gas nitriding of the steel 35CrMo12 by Design of Experiments are in chapter four, followed by chapter five in which the nitrided layer depth is optimized.

Finally, this work is concluded by a general conclusion highlighting the contribution and containing overall interpretation of the performed work as well as perspective for future research.

---

**Chapter One**

**Bibliographic Study on the Diffusion**

**Phenomenon**

---



## I. Chapter One: Bibliographic Study on the Diffusion Phenomenon

### I.1 Introduction

Nitriding studies require knowledge of the diffusion phenomena, since nitrogen atoms are diffused into the material to form nitrided microstructures, as mentioned in the previous chapter.

Hence, in order to study this phenomenon properly, it is necessary to take into account the concepts of diffusion, which is mainly used to improve the mechanical properties of alloys, especially in surface treatments, such as carburizing, boriding, nitriding, etc.

While diffusion may occur in various ways, this work only focuses on that into solid materials, since it is relevant to the study of surface treatment.

### I.2 Definition

The word diffusion comes from the Latin word: *diffusionem*, which means: “a pouring forth”. According to Oxford dictionary, it means: the spreading of something more widely. Another meaning in physics provided by Oxford dictionary is: the intermingling of substances by the natural movement of their particles.

Diffusion is a naturally occurring phenomenon, corresponding to the tendency to spread out of species, particles, atoms or molecules through excitation of energy brought by heat. Depending on the environment in which these species move, the spread will be more or less significant. At room temperature, the diffusion phenomenon will be very significant in a gaseous medium, and less significant in a liquid medium and practically nil in a solid medium. To obtain a diffusion phenomenon in a solid or a crystal, it will be necessary to heat the material to temperatures around 1000°C.

Thanks to the concentration gradient that is established between the external medium (i.e. carbon, boron, etc.) that has a greater concentration than that of the solid medium, the diffusion phenomenon will take place, the movement of atoms is from the highest to the lowest concentration.

Studies concentrated on or relevant to diffusion commonly focus on the determination of the diffusion coefficient, introduced by the German physicist Adolph Fick.

### I.3 Types of Diffusion

Diffusion comes in two different types: auto-diffusion and inter-diffusion. In a solid material, the atoms of the same species also move in the matrix volume. This is the auto-diffusion, as illustrated in Figure I.1.

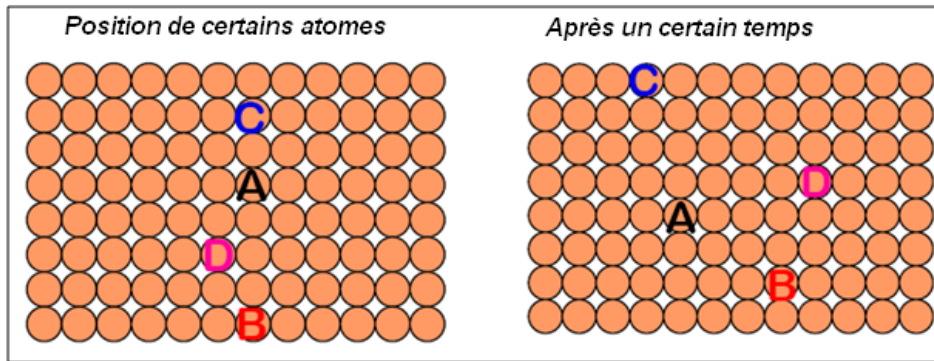


Figure I.1. Auto-diffusion in the same material<sup>[2]</sup>

As for the inter-diffusion, the atoms in an alloy tend to move from regions of high concentration towards regions of lower concentration, as illustrated in Figure I.2.

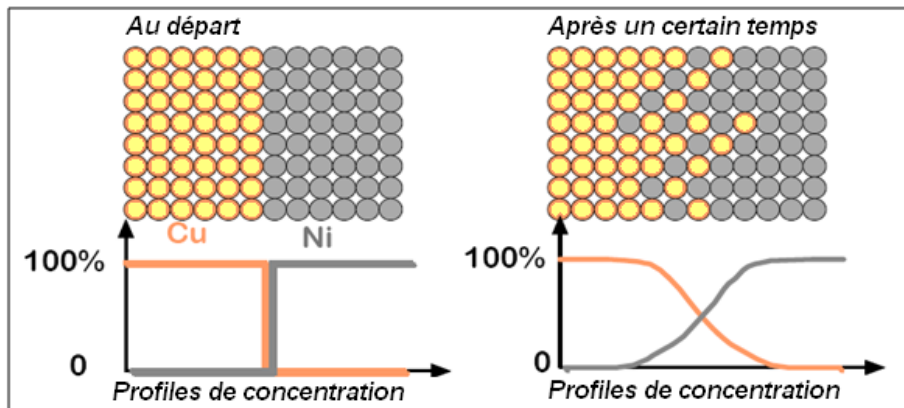


Figure I.2. Pre and post-diffusion concentration profiles<sup>[2]</sup>

### I.4 Diffusion Mechanisms

There are several mechanisms of diffusion, summarized as follows:

- **Interstitial Mechanism:** whereby the solute atoms, which are smaller than the solvent atoms are in interstitial atomic sites, forming thereby an interstitial solid solution. Figure I.3 shows how the solute can jump from an interstitial site to a neighboring site.

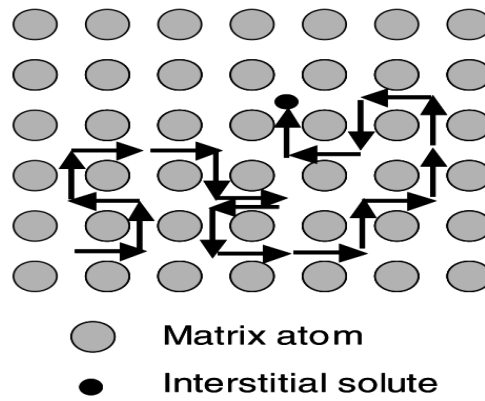


Figure I.3. Direct interstitial mechanism of diffusion<sup>[3]</sup>

- **Collective Mechanisms:** when the solute atoms are similar in size to the host atoms, a substitutional solid solution is usually formed. The mechanism required for such diffusion involves the simultaneous motion of several atoms, as illustrated in Figure I.4<sup>[3]</sup>.

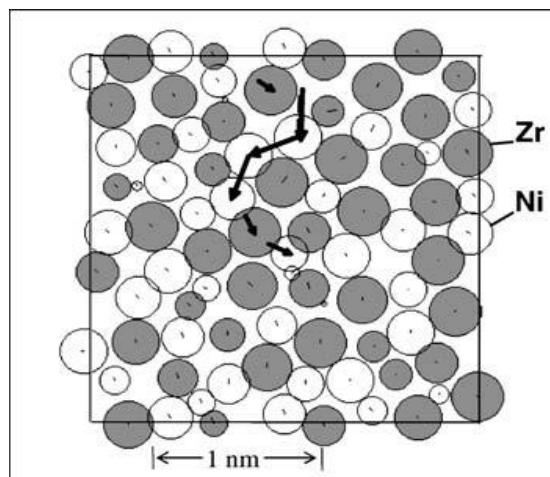


Figure I.4. A simulated motion of atoms chain in an amorphous Ni-Zr alloy<sup>[3]</sup>

- **Vacancy Mechanism:** this is recognized as the dominant mechanism for the diffusion of matrix atoms and of substitutional solutes in metals. A vacancy is a defect in which an atom is missing from one of the lattice sites.

In this mechanism, an atom jumps into a neighboring vacancy, as shown in Figure I.5.

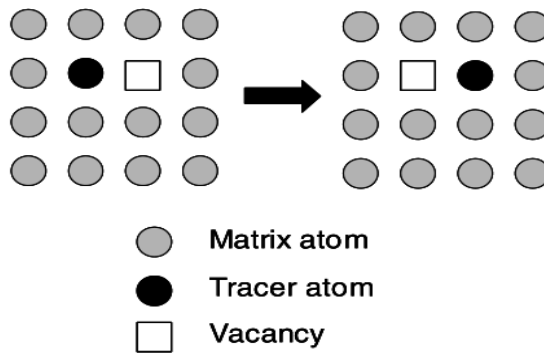


Figure I.5. Monovacancy mechanism of diffusion<sup>[3]</sup>

- **Divacancy Mechanism:** binding energy\* creates agglomerates of vacancies (divacancies, trivacancies, etc.). In this case a diffusion can occur via aggregates of vacancies. Figure I.6 depicts the phenomenon in the case of a divacancy.

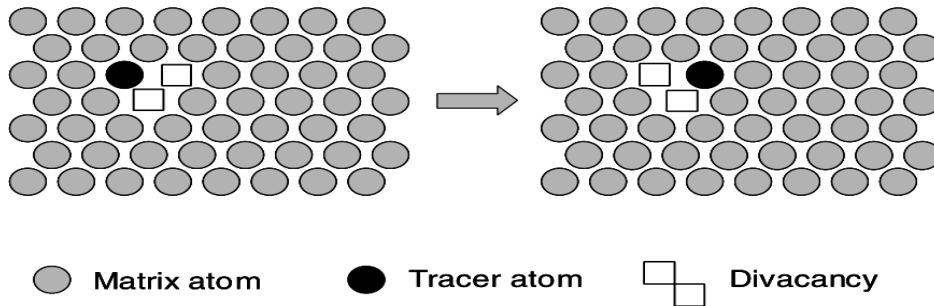


Figure I.6. Divacancy mechanism of diffusion<sup>[3]</sup>

- **Interstitialcy Mechanism:** this mechanism occurs when an interstitial atom is nearly equal in size to the lattice atoms, as depicted in Figure I.7.

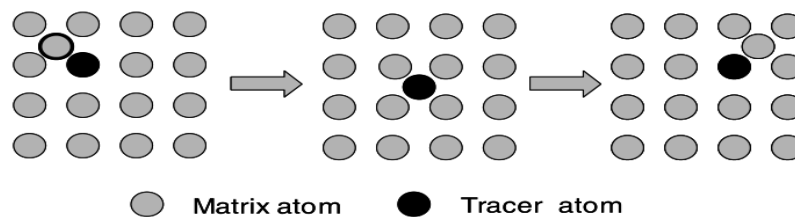


Figure I.7. Interstitialcy mechanism of diffusion<sup>[3]</sup>

- **Interstitial-substitutional Exchange Mechanisms:** these mechanisms occur when a solute atom can be dissolved on both substitutional and interstitial sites of a solvent crystal, as depicted in Figure I.8.

\*The minimum energy required to disassemble a system of particles into separate parts.

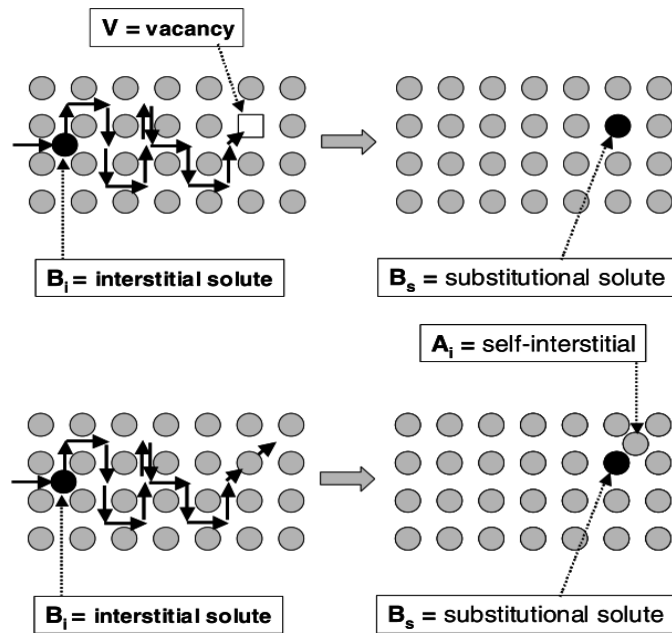


Figure I.8. Interstitial-substitutional exchange mechanisms of foreign atom diffusion<sup>[3]</sup>

## I.5 Diffusion and Temperature

The diffusion coefficient  $D$  is given as a function of temperature by Arrhenius equation as follows:

$$D = D_0 \exp\left(-\frac{Q_d}{RT}\right) \quad \text{I.1}$$

Where  $D$  denotes the diffusion coefficient,  $D_0$  the constant independent of temperature called the frequency factor and  $Q$  the activation enthalpy of diffusion, while  $R$  is the gas constant and  $T$  is the absolute temperature.

The diffusion coefficient is an indicator of the ease with which a substance is diffused within another<sup>[2]</sup>.

## I.6 Fundamental Laws of Diffusion

The two laws of diffusion, formulated in the 19th century by the German physicist Adolph Fick, can be used to model a variety of diffusion problems in binary systems.

- For an isotropic medium, Fick's first law can be formulated as:

$$J_x = -D \frac{\partial C}{\partial x} \quad \text{I.2}$$

Where  $J_x$  is the flux of particles,  $C$  is the concentration of particles and  $x$  is the distance.

This law is illustrated in Figure I.9.

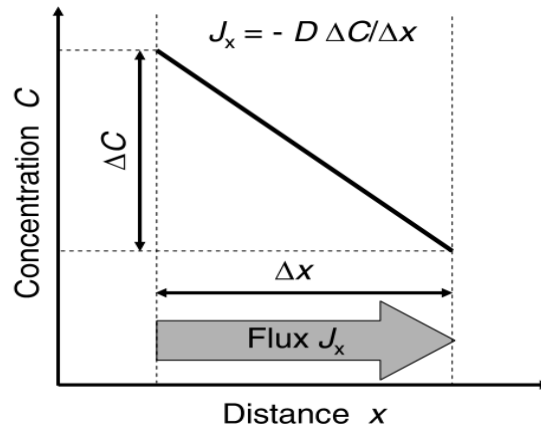


Figure I.9. Illustration of Fick's first law<sup>[3]</sup>

Fick's first law reflects the tendency to spread. The flux of atoms is proportional to the concentration gradient of these atoms<sup>[2]</sup>.

- Fick's second law, also known as the 'Diffusion Equation', is a second-order partial differential equation, given as follows:

$$\frac{\partial C}{\partial t} = \nabla \cdot (D \nabla C) \quad \text{I.3}$$

### I.6.1 Diffusion Equation in Three Dimensions

For an isotropic diffusion, the diffusion equation is written in Cartesian coordinates as:

$$\frac{\partial C}{\partial t} = D \left( \frac{\partial^2 C}{\partial x^2} + \frac{\partial^2 C}{\partial y^2} + \frac{\partial^2 C}{\partial z^2} \right) \quad \text{I.4}$$

Where  $x$ ,  $y$  and  $z$  are the Cartesian coordinates, as presented in Figure I.10.

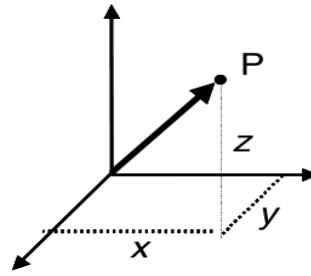


Figure I.10. Cartesian coordinates

## I.6.2 Solutions of the Diffusion Equation

Fick's second (I.3), by which the diffusion phenomenon is governed, admits an analytical solution if  $D$  does not vary over time and is a function of temperature. Hence the solution is:

$$C(x, t) = A \operatorname{erf}\left(\frac{x}{2\sqrt{Dt}}\right) + B \quad \text{I.5}$$

Where  $t$  is the time and  $A$  and  $B$  are constants to be determined according to the boundary and initial conditions, given as follows:

$$\text{Boundary conditions } \begin{cases} C(0, t) = C_s \\ C(\infty, t) = C_0 \end{cases}$$

$$\text{Initial condition } \{C(x, 0) = 0$$

These conditions are illustrated in Figure I.11.

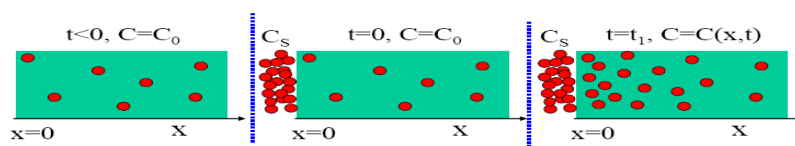


Figure I.11. Boundary and initial conditions of the diffusion equation<sup>[2]</sup>

It should be noted that experiments are often designed in a way to satisfy the initial and boundary conditions.

This equation represents a mathematical model that is used in numerical simulations. According to the aforementioned conditions, the solution of Fick's differential equation is:

$$\frac{C(x, t) - C_0}{C_s - C_0} = 1 - \operatorname{erf}\left(\frac{x}{2\sqrt{Dt}}\right) \quad \text{I.6}$$

It is noticed that the thickness of the diffused layer varies according to time. Figure I.12 presents the values of concentration according to three different diffusion times.

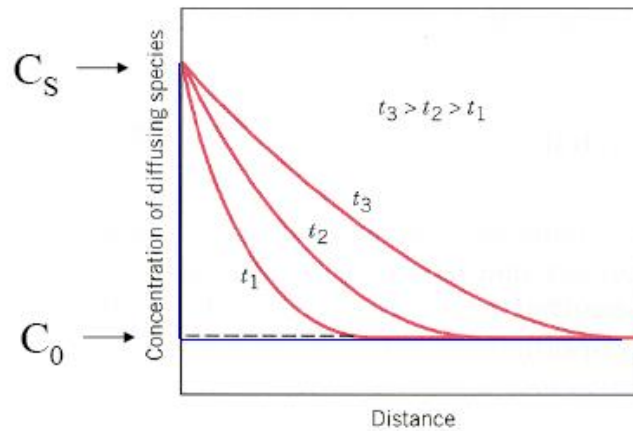


Figure I.12. Concentration profile according to different diffusion times<sup>[2]</sup>

## I.7 Conclusion

This chapter has presented a brief summary of the necessary theoretical concepts of diffusion in materials, as this thesis is not dedicated to the study of diffusion. The most important diffusion laws and equations have been given, along with the different diffusion mechanisms.

Thermal diffusion phenomena in the solid state correspond to jumps made by the atoms in the defects of crystals, under the effect of thermal agitation.

Knowledge of diffusion is indispensable, generally, for materials engineers and scientists who design materials at elevated temperatures as well as at room temperature.



---

# **Chapter Two**

## **Bibliographic Study on Nitriding**

---

## II. Chapter Two: Bibliographic Study on Nitriding

### II.1 Introduction

The nitriding treatment was first developed in the early 1900s, yet before that, the works of the French chemist Edmond Fremy in 1861 proved that it is possible to fix nitrogen on the surface of steel.

Nitriding is often applied to low-alloy steels to improve their mechanical properties, namely hardness, wear resistance and leisure resistance, as well as antiscuffing properties and chemical properties such as corrosion resistance.

Nowadays, nitriding remains a widely used technique in both industrial and research applications, especially in the manufacture of aircraft, bearings and automotive components, as well as textile machinery and turbine generation systems<sup>[4]</sup>.

### II.2 Principle

Nitriding is a surface hardening treatment that is based on the diffusion of nitrogen into the surface of a material, forming thereby nitrides via the solubility of nitrogen in iron along with other alloying elements, if any. The result is a surface layer of about 0.1 mm deep with a hardness approaching 1100 HV<sup>[5]</sup>.

In the case of steels, heat treatment must be applied beforehand, habitually quenching followed by tempering at a high temperature. While the treatment is performed between 500 et 600 °C, the steel in question is quenched and tempered between 550 and 680 °C. The reason for which this tempering temperature interval is chosen is to ensure the stability of the core by avoiding structural evolution during the treatment. Therefore, the tempering temperature is always higher than that of nitriding<sup>[6]</sup>.

### II.3 Nitriding Steels

Nitriding is applied on steels having between 0.3 to 0.4 % of carbon, and containing at least one of the following elements: chromium (Cr), vanadium (V), molybdenum (Mo), aluminium (Al) and titanium (Ti), which have an affinity for nitrogen, thus an ability to form nitrides, such as: Fe<sub>4</sub>N, Fe<sub>2-3</sub>N, CrN, VN, Mo<sub>2</sub>N, Cr<sub>2</sub>N, V<sub>2</sub>N, MoN. These nitrides significantly improve the hardness along with other mechanical and chemical properties.

Nitrogen is added to steels in the ferritic state because it does not require heating into the austenite phase followed by quenching in order to form the martensite, it is rather performed with a minimum of distortion and deformation.

The main families of nitrided steels are the following (according to the Standard **NF A 02-051**):

- Carbon steels C18 to C45;
- 30MnV5 dispersoid steels;
- Chromium molybdenum steels 25CrMo4 to 42CrMo4, 25CrMo12 and 30CrMo12;
- Chromium aluminium molybdenum steels 30CrAlMo6-12, 40CrAlMo6-12;
- Tool steels X38CrMoV5-1, X100CrMoV5, X153CrMoV12;
- Austenitic (X6CrNi18-9, X2CrNiMo17-12) and martensitic (X30 and X40Cr13, X6CrNiMo16-5-1) stainless steels.

### II.4 Phase Diagrams

Determining the nature of the crystalline phases formed during the nitriding of steels requires knowledge of phase diagrams (also called equilibrium diagrams). In practice, thermodynamic equilibrium is certainly not reached; nevertheless, the phase diagrams give an interesting indication of the nature of the phases that can be formed. The iron-nitrogen diagram represents the ranges of existence of metallurgical phases according to nitrogen content and temperature.

#### II.4.1 Binary Diagram Fe-N

The iron-nitrogen diagram in Figure II.1 highlights the presence of the different phases  $\epsilon$ ,  $\gamma'$  and  $\alpha$ , i.e. three single-phase domains:

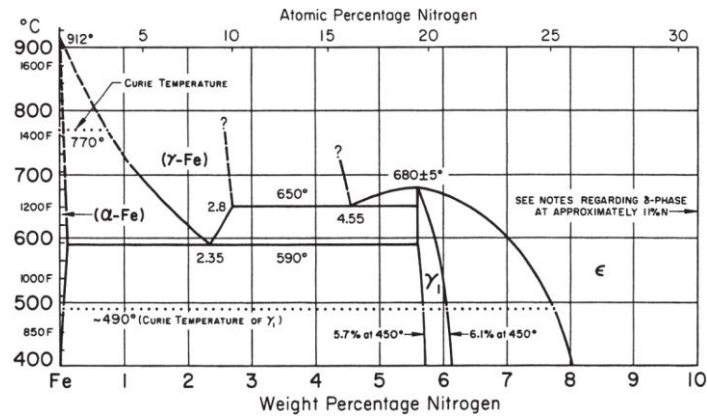


Figure II.1. Iron-nitrogen equilibrium diagram<sup>[4]</sup>

- **Solid solution α** of nitrogen in iron with very low solubility in nitrogen (<0.1%*m*). After exceeding this percentage, iron nitrides ε or γ' are formed, according to the mass fraction of nitrogen<sup>[7]</sup>.
- **Nitride γ'** (Fe<sub>4</sub>N) of face-centered cubic structure (CFC) in which a nitrogen atom occupies the octahedral site in the lattice center (Figure II.2). This nitride is stable in a range of composition at 590 °C, which ranges from 19 to 20.2 atoms % of nitrogen, i.e. 5.5 to 5.75% by mass. Its hardness is about 800 HV.

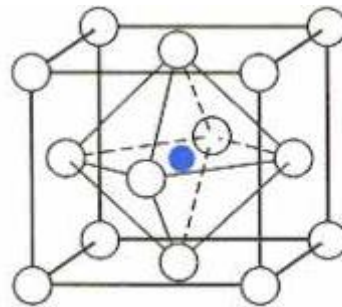


Figure II.2. Structure of the nitride γ'<sup>[11]</sup>

Iron FCC lattice with a nitrogen atom in the octahedron. There are therefore 4 iron atoms and one nitrogen atom per elementary cell<sup>[11]</sup>.

- **Nitride ε** of compact hexagonal structure (HC) whose octahedral sites are occupied by quantities of nitrogen atoms that are variable according to the composition of the nitride (Figure II.3). Its formula is of the type Fe<sub>2-3</sub>N.

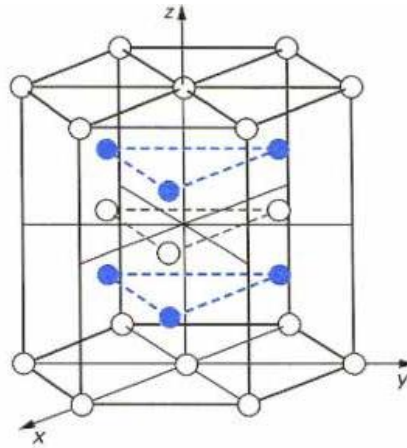


Figure II.3. Nitride structure  $\text{Fe}_2\text{N}-\text{Fe}_3\text{N}$ <sup>[11]</sup>

This nitride is an extensive solid solution of nitrogen in iron. It corresponds to the compact hexagonal structure of the iron network. The elemental lattice of the stoichiometric  $\text{Fe}_3\text{N}$  nitride comprises:

$$\left(4 \times \frac{1}{6} + 4 \times \frac{1}{12} + 1\right) \times 3 = 6 \text{ iron atoms and 2 nitrogen atoms.}$$

Depending on the fill rate of the available octahedral sites of the lattice, it goes from  $\text{Fe}_4\text{N}$  to  $\text{Fe}_2\text{N}$ : the illustrated lattice corresponds to  $\text{Fe}_3\text{N}$ <sup>[11]</sup>.

#### II.4.2 Ternary Diagram Fe-N-C

Since nitriding is a generally applied on steels, studying the effect of carbon is highly important. The binary diagram Fe-N is insufficient to study the nature of the formed phases in the nitriding of unalloyed steels. It is thus better to use the ternary diagram Fe-N-C. It should be noted that the presence of carbon promotes the formation of the nitrides  $\epsilon$ , particularly at temperatures around 565 °C<sup>[7]</sup>.

Considering the temperature 580 °C, Figure II.4 illustrates an isothermal cut of the Fe-N-C phase diagram. The following observations are made:

- Nitrogen is poorly soluble in iron carbides. Its solubility is practically nil in cementite  $\text{Fe}_3\text{C}$  and reaches 0.5% by mass in Hägg carbide  $\text{Fe}_7\text{C}_3$ ;
- Carbon is hardly soluble in  $\gamma'$  nitride, its maximum solubility is less than 0.2% by mass;
- The nitride  $\epsilon$  has a very wide range of existence. At the temperature of 565 °C, the solubility limit of carbon is 3.7 % by weight (carbon occupies the octahedral

sites left vacant by nitrogen). There is then a phase called carbonitride  $\epsilon$  of formula  $\text{Fe}_{2-3}(\text{C,N})$  [7].

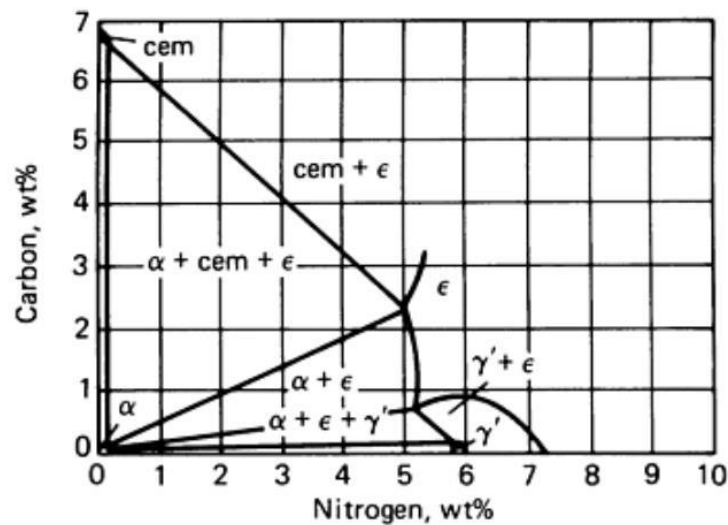


Figure II.4. Isothermal cut at 580°C of the Fe-N-C equilibrium diagram<sup>[8]</sup>

The carbon in steel also plays a role on the nature of the layer obtained: the higher the carbon content of the matrix, the less external input is required. Yet an excess of carbon can lead to the formation of cementite, which blocks the kinetics of nitride formation<sup>[10]</sup>.

### II.4.3 Complex Diagram Fe-N-C-X

In industry, nitriding is generally applied to steels containing alloying elements that can form nitrides with atomic nitrogen, i.e. nitriding elements such as chromium, molybdenum, aluminium and vanadium. Nitriding of steels reveals the existence of several carbides, nitrides and iron carbonitrides, and other alloying elements in which nitrogen and carbon are inserted.

Therefore, the study of Fe-N and Fe-N-C equilibrium diagrams is not sufficient to understand all the phenomena involved in the nitriding of alloy steels. Hence, it is necessary to study the phase diagrams between nitrogen and all the elements contained in the alloy.

A study conducted by Guerrero for the steel XC18, nitrided at 550 °C, has shown that the diffusion of nitrogen in steels is accompanied by a retrodiffusion of carbon as it is driven to the material's core<sup>[9]</sup>. Figure II.5 illustrates this result.

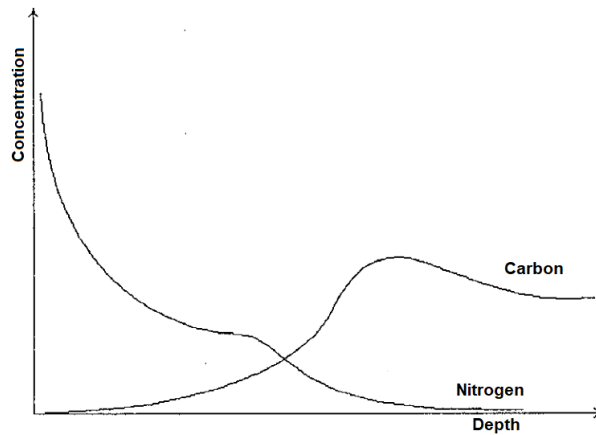


Figure II.5. Nitrogen and carbon concentrations as function of depth for a nitrided steel<sup>[9]</sup>

Another graph plotted by Guerrero shows the effect of nitrogen and carbon profiles on the microstructure, according to each zone of the nitrided steel, as shown in Figure II.6.

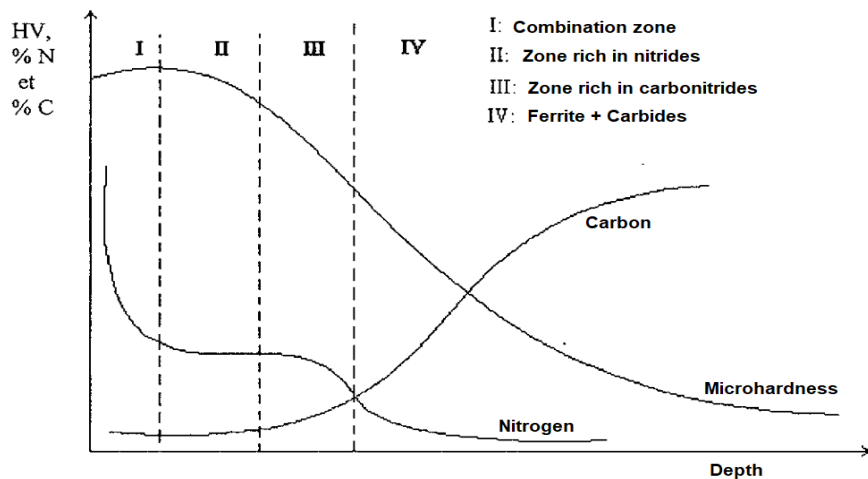


Figure II.6. Effect of nitrogen and carbon profiles on the microstructure of a nitrided steel<sup>[9]</sup>

A simple observation of this graph shows that the microhardness is decreasing with the content of nitrogen in the steel, as function of the depth.

## II.5 Structures of The Formed Layers

The solubility of nitrogen in iron can form a solid solution with ferrite at about 6% N, where the compound  $Fe_4N$  ( $\gamma'$ ) is formed, while at nitrogen contents greater than 8%, the reaction product is  $Fe_3N$  ( $\epsilon$ )<sup>[6]</sup>.

This diffusion leads to the formation of two layers of different structures: the compound layer and the diffusion (nitrided) layer, as shown in Figure II.7, Figure II.8 and Figure II.9.

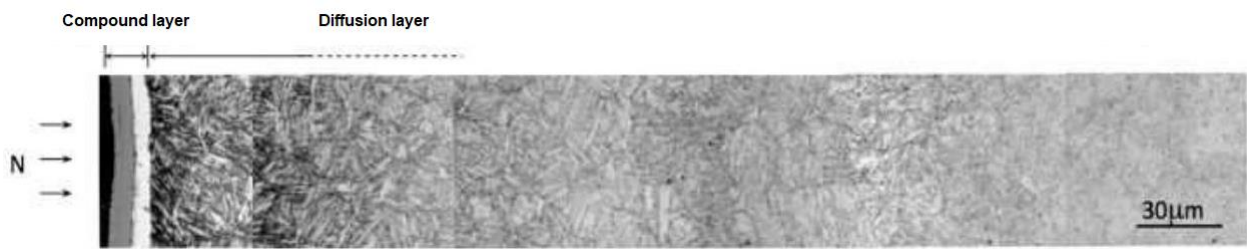


Figure II.7. Microstructure of the nitrided zone of a steel<sup>[8]</sup>

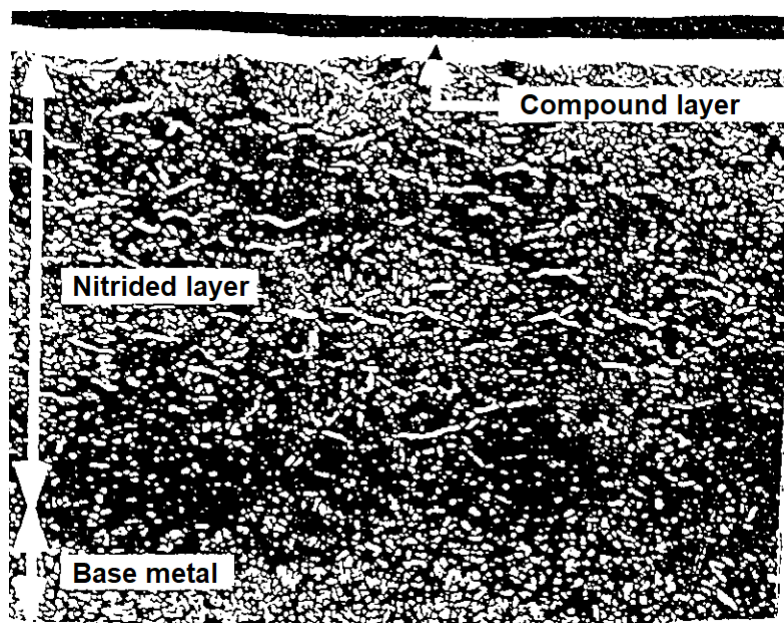


Figure II.8. Micrograph of the nitrided layer of steel 32CrMoV13. Nital attack 3%<sup>[7]</sup>



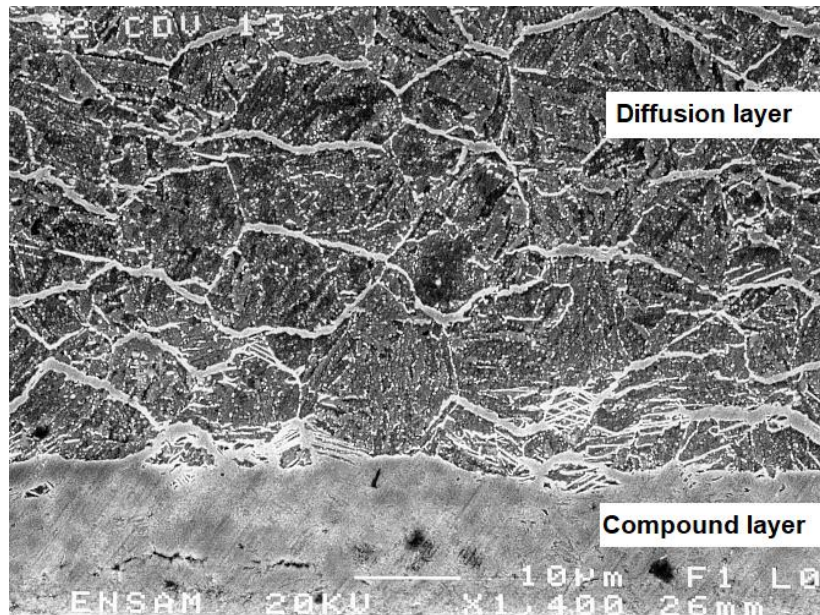


Figure II.9. M.E.B. micrograph of the nitrided layer of the steel 32CrMoV13<sup>[10]</sup>

### II.5.1 The Compound Layer

This is a single-phase or two-phase white\* layer ( $\epsilon$  or  $\gamma'$  or both), where  $\epsilon$  is  $\text{Fe}_{2-3}\text{N}$  of HC structure (see Figure II.3) and  $\gamma'$  is  $\text{Fe}_4\text{N}$  of CFC structure (see Figure II.2). The white layer is undesirable: despite its hardness, it is highly brittle that it may spall in use, thus special nitriding processes are applied to reduce this layer or make it less brittle. However, it is proven that this structure increases wear resistance<sup>[6]</sup>.

The thickness of the white layer strongly depends on the nitriding parameters as well as the composition and initial microstructure of the steel.

It should be noted that in the case of gas nitriding, this layer is always two-phase,  $\epsilon + \gamma'$ , whereas  $\epsilon$  is to a larger extent<sup>[8]</sup>.

Depending on the nitriding conditions and the base material used, the following is obtained:

- A total absence of the white layer for the low contents of nitrogen;
- A single-phase layer  $\gamma'$  (if the nitrogen concentration is maintained at a sufficiently low level) or almost a single-phase  $\epsilon$  (high nitrogen concentration at 570 °C). It is difficult to obtain such layers if the nitriding potential is not well controlled;

\* Because of the color it obtains after being exposed to natal.

- A mixture of the phases  $\epsilon$  and  $\gamma'$  in proportions that vary depending on the operating conditions.

### II.5.2 The Nitride $\text{Fe}_4\text{N}_{2-3}$

This nitride (depicted in Figure II.2) is the first to form in the iron nitride series because it precipitates at low temperatures and requires only a local nitrogen content of around 20 atomic %. Its affinity for carbon is also very low since only 0.2 mass % of carbon can be dissolved in its structure. In addition, this phase improves resistance to cracking<sup>[8]</sup>.

### II.5.3 The Nitride $\text{Fe}_4\text{N}_{2-3}$

This nitride (depicted in Figure II.3) has a large compositional range from 8.25 to 11% by mass of nitrogen. It is most often referred to as carbonitride  $\epsilon$  because of its high affinity for carbon; the carbon content in this phase can be as high as 3% by mass. It is a way to obtain single-phase combination layers  $\epsilon$  by ion nitriding. In addition, many authors agree on the high hardness and good tribological properties of this phase and its increased ductility compared to the  $\gamma'$  phase. It also improves wear resistance by avoiding certain adhesion problems<sup>[8]</sup>.

### II.5.4 The Diffusion Layer

The arrival of nitrogen atoms in the diffusion layer leads to the insertion of nitrogen into ferrite and the precipitation of nitrides in ferrous alloys or steels. Depending on the processing conditions and the chemical nature of the alloy, the depth of nitriding can vary from a few hundred microns to one millimeter. This layer is constituted of nitro ferrite, nitrides and carbonitrides. The thickness of this layer is between 300 and 800  $\mu\text{m}$ . The solubility limit of nitrogen in the ferritic matrix turns out to be very low (0.043%N at 520°C), as a consequence of a very limited insertion in the centered cubic network of the matrix. This insertion has only a small impact on the mechanical properties compared to that of the precipitates<sup>[8]</sup>.

This layer improves the endurance limit, due to the increase in hardness and the presence of compressive stress. Compressive stresses originate in the surface layers, which change in volume due to the insertion of nitrogen, while the non-nitrided core does not change<sup>[7]</sup>.

The hardness of both layers (compound and diffusion layers) as function of depth is illustrated in Figure II.10.

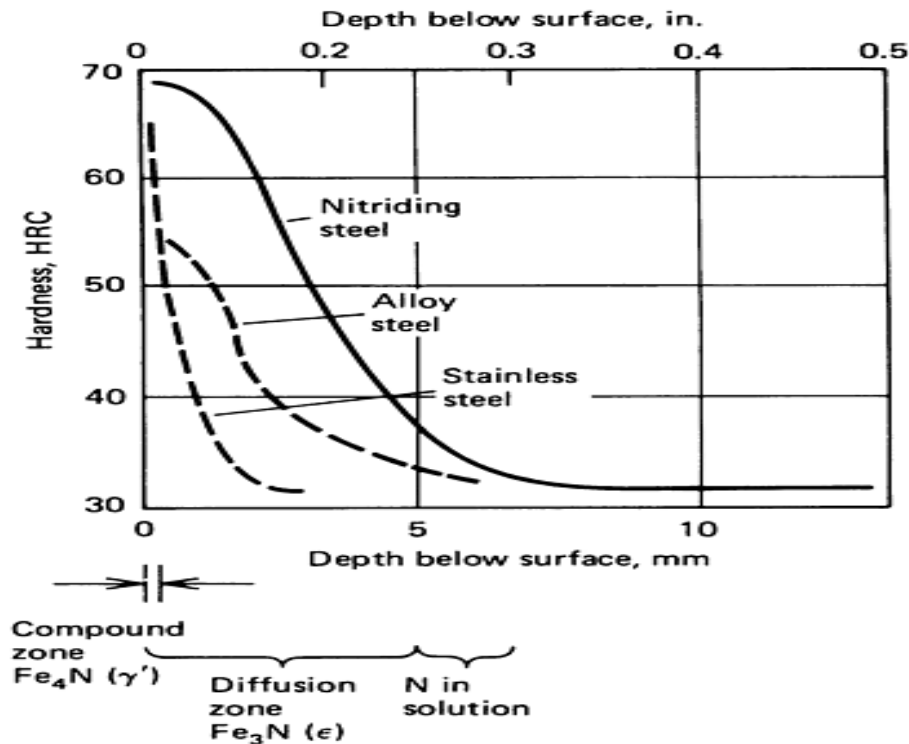


Figure II.10. Nitride case profiles for various steels<sup>[6]</sup>

## II.6 Enthalpy of Formation

As aforementioned, in order to have a hardening phenomenon in ferrous alloys, the latter must contain elements capable of forming nitrides with diffused nitrogen. These nitrides lead to a structural hardening that results in an improvement of the endurance limit due to an increase in surface hardness. The nitrides formed are those that have the highest enthalpy of formation ( $\Delta H^{298}$ ) in absolute value.

Table II-1 below lists the nitrides that may be formed from the addition elements. The choice of nitriding steels is based on steels that do not contain Nickel since Nickel does not form nitrides.

Phases	Bravais lattice	Enthalpy of formation $\Delta H^{\circ}_{298} \text{KJ/Mole}$	Lattice parameters $\text{A}^{\circ}$
Fe <sub>2-3</sub> N	HC	-3.76	a=4.787 b=4.422
Fe <sub>2</sub> N	Orthorhombic	--	a=5.524 b=4.827 c=4.422
Fe <sub>4</sub> N	CFC	-10.9 ± 8.4	a=3.79
Mo <sub>2</sub> N	CFC	-69.4 ± 2.1	a=4.169
Cr <sub>2</sub> N	HC	-105.3 ± 12.6	a=4.796 b=4.47
CrN	CFC	-118 ± 10.5	a=4.149
Mn <sub>4</sub> N	CFC	-130.4 ± 12.6	a=3.865
VN	CFC	-251 ± 21	a=4.169
AlN	Hexagonal	-320 ± 4.2	a=3.104 b=4.965
TiN	CFC	-336 ± 3.3	a=4.237
Si <sub>3</sub> N <sub>4</sub>	Hexagonal	-748 ± 33.4	a=7.748 b=5.617
Fe <sub>16</sub> N <sub>2</sub>	Centered quadratic	--	--

**Table II-1. List of nitrides that may be formed from addition elements<sup>[11]</sup>**

Hence it is possible to predict the formation of nitrides or carbides from the standard enthalpies of formation  $\Delta H^{\circ}_f(x)$  of these compounds, since nitriding obeys the laws of thermodynamics and the phases observed in nitrogen-affected areas can be predicted by the thermodynamics of the system.

## II.7 Influence of Alloying Elements

The choice of a steel to be nitrided must be made according to the desired characteristics of the part and the conditions under which it is made.

The selection criteria are divided into two groups:

- Characteristics of the core (strength, hardenability, heat resistance, weldability, etc.);
- Characteristics of the nitrided layer (hardness, brittleness, depth, etc.).

Nitriding of non-alloy steels is of little interest, as surface hardness is only of the order of 100 HV with an improvement in the coefficient of friction but with a risk of embrittlement.

The main hardening elements in decreasing order are: aluminium, chromium, titanium, molybdenum, vanadium and manganese<sup>[11]</sup>.

Figure II.11 shows the evolution of the nitrogen-alloying elements activity coefficients  $f_N^X$  as a function of the content of the alloying elements. These values characterize the effect of the element X on the solubility of nitrogen in ferrite. Elements with a negative gradient of the activity coefficient (Ti, V, Mn, Mo, Cr, W) tend to increase the solubility of nitrogen in ferrite.

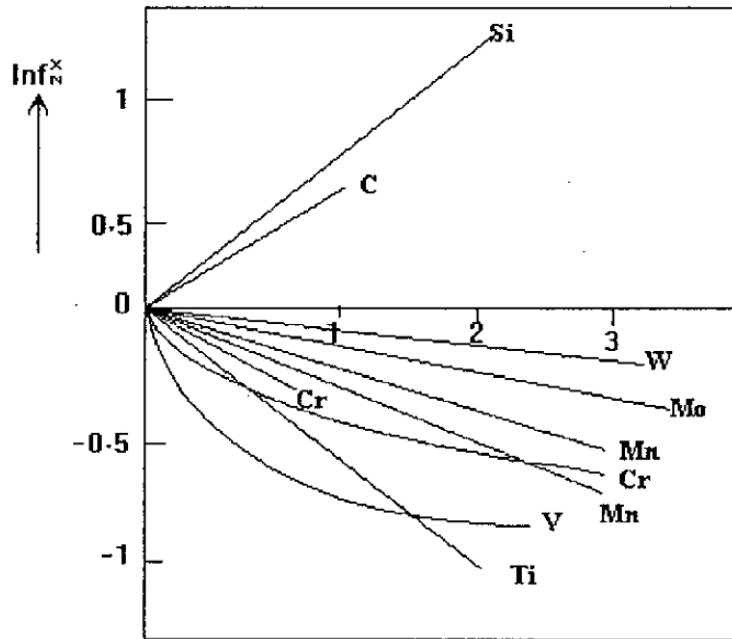


Figure II.11. Effect of alloying elements on the activity coefficient of nitrogen in iron at 500 °C [9]

The interaction between the alloying element X and nitrogen defines the mode of precipitation. According to a study conducted on Fe-Cr, Fe-Ti, Fe-Mo and Fe-Al, nitrided at 575 °C, in gaseous phase, and from the microhardness profiles, there are three modes of nitrogen-metal element interaction:

- **Strong interaction** (Figure II.12.a): characterized by a strong precipitation of the nitride XN in the entire nitrogen-rich zone. Case of: Fe-Cr at Cr > 5%, Fe-V at V > 1% and Fe-Ti at Ti > 2%;
- **Weak interaction** (Figure II.12.b): most of the nitrogen is dissolved in the ferrite, there is only a slight precipitation of nitrides of these elements. Case of: Fe-Cr at Cr = 1-2% and Fe-Mo at Mo < 5%;

- **Mean interaction** (Figure II.12.c): it is an intermediate interaction mode between the two previous cases, one can find as much free nitrogen in the matrix as fixed by the nitride<sup>[9]</sup>.

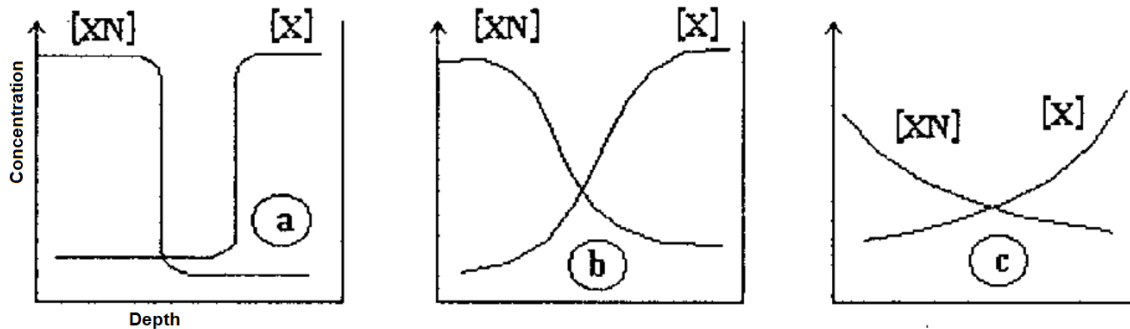


Figure II.12. Mode of interaction between alloying elements and nitrogen<sup>[9]</sup>

### II.7.1 Influence of Aluminium

Aluminium is the most hardening element in the nitrided layers as the surface hardness increases with the increase in aluminium content in the nitrided steel. Too high content of aluminium leads to a lack of hardness progression from the surface to the core, thus rendering the parts sensitive to chipping.

The high reactivity and low density of aluminium makes its addition a delicate process and leads to the formation of inclusions that can sometimes be detrimental to both mechanical characteristics and polishability<sup>[10]</sup>.

### II.7.2 Influence of Chromium

It plays a major role in surface hardening and in improving some characteristics of steels by increasing its hardenability.

For contents higher than 4%, it reduces the reactivity of the surface to nitriding and requires the use of processes that activate the surface<sup>[10]</sup>.

### II.7.3 Influence of Molybdenum

Molybdenum increases the hardenability of steel and reduces embrittlement on tempering. It also contributes significantly to surface hardening<sup>[10]</sup>.

### II.7.4 Influence of Nickel

Nickel is widely used to increase the hardenability of steels. In the case of nitriding, attention must be paid to the risk of tempering embrittlement that most steels with nickel as the main alloying element present<sup>[10]</sup>.

### II.7.5 Influence of Vanadium

Vanadium is involved in surface hardening. The point of using it is to limit grain growth during pre-nitriding treatments and to increase resistance to tempering softening; it limits the reduction in mechanical characteristics by the tempering effect during nitriding<sup>[10]</sup>.

## II.8 Nitriding Types

Nitriding can be classified in two ways: considering the solute-solvent interactions, or considering the used technique.

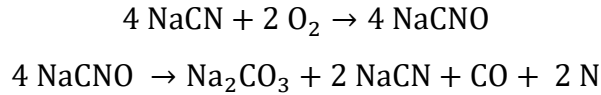
The interactions between the solute and solvent define three temperature domains:

- **High Temperature Nitriding:** the alloying elements (Ti, V, Mo, Nb, Ta, Cr, W, Mn) move easily through the steel matrix, and the nitrides of the alloying elements precipitate.
- **Nitriding at Medium Temperature:** the alloying elements move at a short distance except for nitrogen, which moves at a long distance.
- **Low Temperature Nitriding:** at  $T < 350$  °C, most of the substitutional alloying elements are immobile.

Considering the used technique, there are four types of nitriding: solid nitriding, liquid nitriding plasma nitriding and gas nitriding.

- **Solid Nitriding:** the saturation agent in this operation is a powder rich in nitrogen, boron and carbon. Calcium cyanamide is the nitriding agent in the presence of activators that release the elements N, C, O and H. The parts are placed in welded steel or sometimes cast iron boxes. The solid nitriding temperature varies between 500 and 590°C. After nitriding, the boxes are opened and cooled in the open air.

- **Liquid Nitriding:** in this type of nitriding, molten salt baths are used at 570 °C (alkaline cyanide), applicable to alloy steels and alloy nitriding steels. The supply of nitrogen is due to the decomposition of the cyanates formed by oxidation of the cyanides:



- **Plasma Nitriding:** plasma nitriding process began in the 1920's as an alternative to conventional gas nitriding. It allows the introduction of nitrogen from the ions of a plasma obtained by electrical discharge into a mixture (N<sub>2</sub> + NH<sub>3</sub>) at low pressure close to three torr (133.32 Pa)

The following table summarizes the four types of nitriding:

Process	Nitriding Agents	T (°C)	T (h)	Advantages	Disadvantages
Solid Nitriding	Cyanamide + Calcium + Activator	470 à 570 °C	1 à 25 hours	<ul style="list-style-type: none"> <li>• Simplicity</li> <li>• Security</li> </ul>	<ul style="list-style-type: none"> <li>• Small parts</li> <li>• Not very mechanizable</li> </ul>
Liquid Nitriding	Cyanides + Cyanates + Carbonate	570 °C	1 à 5 hours	<ul style="list-style-type: none"> <li>• Short and inexpensive treatment</li> <li>• Simplicity</li> <li>• Easy, economical implementation</li> </ul>	<ul style="list-style-type: none"> <li>• Pollution</li> <li>• Not very mechanizable</li> <li>• Fixed processing temperature</li> <li>• Cleaning of parts after treatment</li> </ul>
Plasma Nitriding	Ammonia or Nitrogen or Nitrogen + Methane	350 à 600 °C	0.25 à 40 hours	<ul style="list-style-type: none"> <li>• Low energy consumption</li> <li>• Cleanliness</li> <li>• Automation possibility</li> <li>• Good control of the nature of the surface layer</li> </ul>	<ul style="list-style-type: none"> <li>• Expensive equipment and treatment</li> <li>• Low loads</li> <li>• Nitriding of parts with complex geometry</li> </ul>
Gas Nitriding	Ammonia or Ammonia + Gas	510 à 570 °C	10 à 100 hours	<ul style="list-style-type: none"> <li>• Big parts</li> <li>• Easy to implement</li> <li>• Inexpensive</li> </ul>	<ul style="list-style-type: none"> <li>• Long treatment</li> <li>• Toxic gas</li> <li>• High gas consumption</li> </ul>

Table II-2. Comparison between the different types of nitriding<sup>[10]</sup>

## II.9 Gas Nitriding

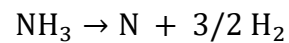
Gas nitriding was discovered in 1923 by a technician of the firm Krupp who, after heating a steel in an ammonia atmosphere, observed an abnormally high surface hardness. In recent years, gas nitriding remains one of the most utilized surface engineering techniques and the most popular nitriding type, due to its excellent applicability to a wide



range of steel grades, in addition to the small dimensional changes it causes to the nitrided workpieces, not to mention the various improvements it brings to mechanical properties.

Anhydrous ammonia gas ( $\text{NH}_3$ ) is injected into a sealed metal muffle furnace (pot furnace or bell furnace) with perfect mixing of atmosphere and high temperature accuracy:  $\pm 3$  °C<sup>[11]</sup>.

The part to be treated is placed in a furnace, exposed to atmosphere containing ammonia. The purpose is to release the atomic nitrogen, by the chemical reaction:



The atomic nitrogen is first absorbed by the surface, and diffuses into the material thereafter.

Figure II.13 shows a tempering furnace, while Figure II.14 shows a gas nitriding furnace.



Figure II.13. Tempering furnace<sup>[8]</sup>

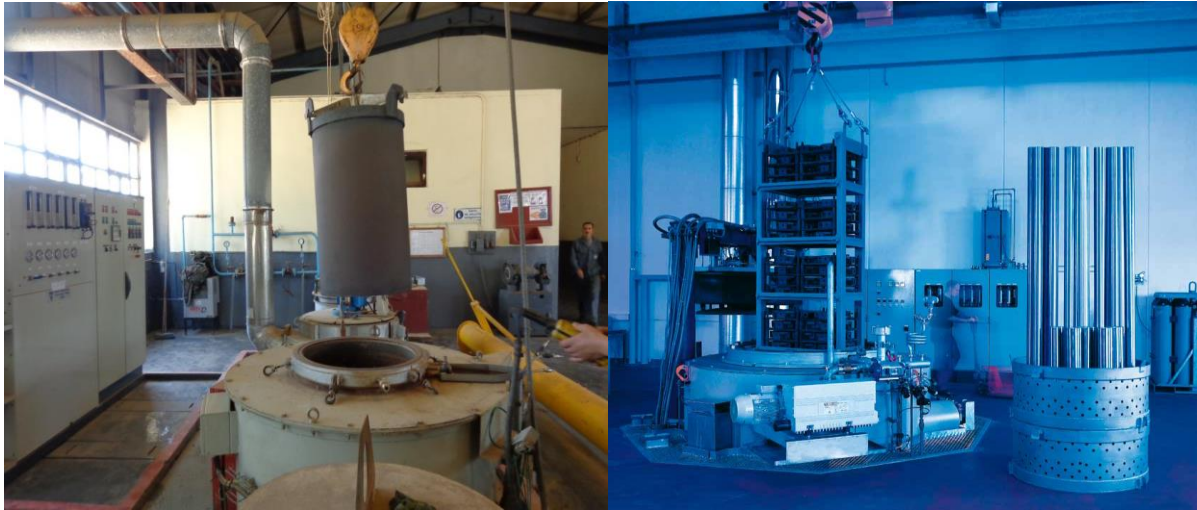


Figure II.14. Gas nitriding furnace<sup>[9][12]</sup>

### II.9.1 Gas Nitriding Fundamental Factors

The gas nitriding treatment is characterized by several parameters, primarily the following:

- **Temperature**

Temperature plays an important role in the mechanical properties of nitrided surfaces, an increase in temperature leads to:

- An increase in the depth of the diffusion layer and an increase in the thickness of the combination layer;
- An increase in the hardness of the diffusion zone up to a critical temperature, which depends on the steel grade, beyond which the hardness decreases;
- This results in a decrease of the maximum compressive stress and a displacement of the nitriding depth where this maximum is located, towards the core of the material<sup>[13]</sup>.

- **Time**

The increase in treatment duration leads to an increase in the depth of the nitrided layer. The nitriding time influences the residual stresses. The maximum compressive

stress has a nearly constant value and moves toward the inside of the material when time increases<sup>[13]</sup>.

- **Diffusion Rate of Ammonia**

In a nitriding treatment, for a fixed time and temperature, the increase in the rate of dissociation of ammonia results in:

- A decrease in the thickness of the combination layer;
- A displacement of the nitriding position from the maximum compressive stress to a nearly constant value<sup>[13]</sup>.

The diffusion rate of ammonia is given as follows:

$$\tau = \frac{\text{Volum of NH}_3 \text{ transformed into N}_2 \text{ and H}_2}{\text{Volum of NH}_3 \text{ used}} \quad \text{II.1}$$

This ratio gives the quantity of ammonia that participates in the nitriding treatment.

- **Nitriding Potential**

The nitriding potential  $K_n$  is also important in this treatment, it is defined as follows:

$$K_n = \frac{P(\text{NH}_3)}{P(\text{H}_2)^{3/2}} \quad \text{II.2}$$

This potential defines the possibility of creating the nitrogen layers of determined structure. In general, the higher the potential is, the resulting phases are richer in nitrogen.

If  $K_n$  is multiplied by the equilibrium constant  $K$ , the concentration of the dissolved nitrogen is obtained:

$$[\text{N}] = K \frac{P(\text{NH}_3)}{P(\text{H}_2)^{3/2}} \quad \text{II.3}$$

- **Pressure**

Figure II.15 illustrates a protocol for gas nitriding under different pressure values. It was found that by performing gas nitriding under pressures ranging from 1 to 6 atm, the treatment's kinetic process was accelerated and the rapid thickness of the nitrided

layers was promoted compared to conventional gas nitriding under 1 atm pressure. In addition, gas nitriding performed under 6 atm for 5h exhibited the best wear resistance, with a thickness of 410  $\mu\text{m}$ , which is almost equal to that of conventional gas nitriding, 440  $\mu\text{m}$ , performed for 50h. the temperature in both cases was 510  $^{\circ}\text{C}$  [14].

The steel used in the aforementioned investigation was 38CrMoAlA.

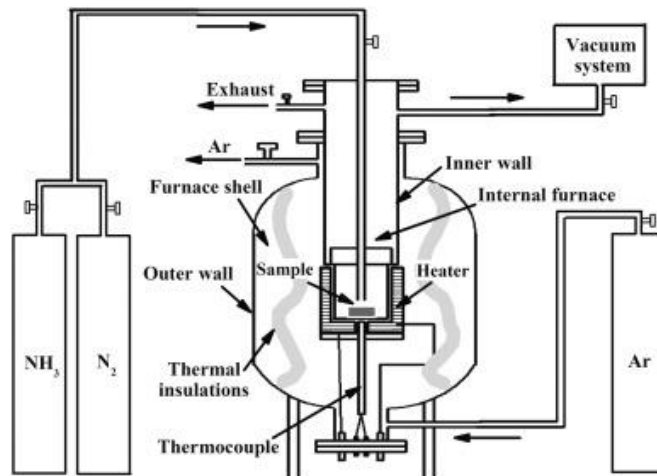


Figure II.15. Pressurized gas nitriding scheme<sup>[14]</sup>

## II.10 Conclusion

This chapter has presented the nitriding treatment from several angles. The types of nitriding have been cited, the nitriding parameters clarified, and the relevant phenomena explained.

It is noteworthy that although the nitriding mechanism is generally known, the reactions that occur throughout the process are not always known, thus the types of nitrides that may be formed cannot be determined beforehand. Therefore, nitriding studies usually require the use of simulation software.

Gas nitriding is fairly one of the most used of nitriding types. Several parameters influence this treatment, yet usually only three of these are considered in experimental and simulation studies, which are temperature, time and potential.

---

**Chapter Three**

**Bibliographic Study on Design of**

**Experiments**

---

### III. Chapter Three: Bibliographic Study on Design of Experiments

#### III.1 Introduction

Classical experimental strategies consist of successively varying one factor in each and every experience, which is called one factor at a time approach. Yet this is a costly and time consuming method, because determining the parameters that are directly responsible of the changes in the system requires performing the experience many times. In order to minimize the number of factors used in experimentation, engineers use their prior knowledge and even intuition.

In the 1920, Sir Ronald A. Fisher first introduced the Design of Experiments (DoE) as an optimization method. Although he used this method in the agricultural research, researchers have since developed the method and its applications in various fields<sup>[15]</sup>.

Design of experiments (DoE) is a systematic, rigorous approach to engineering problem-solving that applies principles and techniques at the data collection stage so as to ensure the generation of valid, defensible, and supportable engineering conclusions. In addition, all of this is carried out under the constraint of a minimal expenditure of engineering runs, time, and money<sup>[18]</sup>. The DoE thus allows to acquire the maximum of information with a minimum number of experiences<sup>[16]</sup>. Generally, wherever an experiment exists, there is a possibility of implementing a DoE analysis.

A fine research work should be bound by the following logical scientific learning cycle:

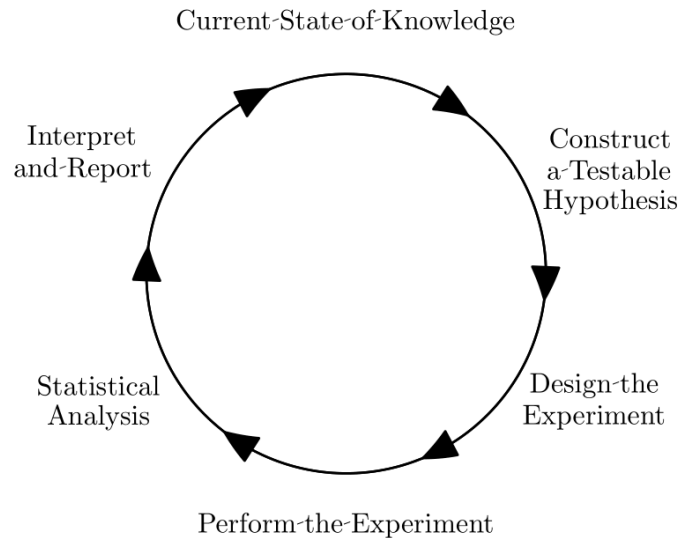


Figure III.1. The circular flow of scientific learning<sup>[17]</sup>

The DoE can be also utilized as a modeling method, provided the existence of a sufficient amount of experimental data.

### III.2 Experimental Design Objectives

The main types of experimental designs are listed below according to the experimental objectives to which they respond:

- **Comparative objective:** if you have one or more factors under investigation, but the main purpose of your experiment is to draw a conclusion about a factor that is important a priori, (in the presence and/or despite the existence of the other) factor(s)), and the question that arises is whether or not that factor is "significant" (i.e. whether or not there is a significant change in response for different levels of that factor), then you have a comparative problem and a comparative design solution;
- **Screening Objective:** the main purpose herein is to select or filter the few important main effects from the many less important ones. These screening designs are also called main effects designs;
- **Response surface:** this consists of designing the study to allow for estimating the interaction and even quadratic effects, and thus giving an idea of the (local) shape of the response surface under study. For this reason they are called response surface method (RSM) designs. RSM designs are used for:



- Finding improved or optimal process parameters;
- Solve process problems and weaknesses;
- Making a product or process more robust against external and uncontrollable influences. Robust means relatively insensitive to these influences;
- **Optimal fit of a regression model:** when the aim is to model a response as a mathematical function (known or empirical) of a few continuous factors and good estimates of model parameters (i.e. unbiased and minimal variance) are required, then a regression design is needed<sup>[18]</sup>.

### III.2.1 DoE Advantages

The efficiency of scientific experiments is often imposed. According to an estimation made by J. Bernal, scientific research is mostly chaotic to the point of having a coefficient of usability of about 2%<sup>[19]</sup>. Thence, the DoE was developed to increase research efficiency.

The methodology of Design of Experiments brings the following advantages:

- Reducing or minimizing the total number of trials of a given experiment;
- Simultaneous varying of all factors that formalize the experimenter's activities;
- Choice of a clear strategy that enables reliable solutions to be obtained after each sequence of experiments;
- Benefiting from existing experimental data by creating a DoE model.

The purpose is thus acquiring the maximum amount of information with a minimum expenditure of time and resources. Using the DoE, the consumption of research time may be reduced ten or more times. Taking the example of an experiment with five factors, each of which may be varied at five levels. In order to study all the possible variations, that is to test the research subject completely, it is necessary to perform  $5^5=3215$  different experiences. Nevertheless, it is possible to use the DoE and perform only 25 trials<sup>[19]</sup>.

### III.3 Implementing a Design of Experiments

In order to execute a DoE analysis in a given phenomenon, there are three things that must be determined:

- The response, which is measurable result that the study aims to analyze and/or improve;
- The factors, which are the analyzed variables that can affect this response;
- The levels, which are concrete values of each factor that should be tested.

In order to acquire valid statistical inferences, the following questions must be answered:

- How to measure the response and the factor's effect?
- How many of the factors will affect the response?
- How many of the factors will be considered simultaneously?
- How many repetitions of the experiment will be required?
- What type of data analysis is required?
- What level of difference in effects is considered significant?

A study with  $p$  levels and  $k$  factors would require  $p^k$  experiences

### Example of a $2^4$ study

Considering a paper airplane with 4 factors, each of which has 2 levels, given as follows:

- Height (high/low): the height from which the paper airplane will be released;
- Speed of wind (60/75): the speed of wind into which the paper airplane will be released;
- Air resistance (5/15);
- Material of which the paper airplane is made (paper/cardboard).

If the desired response is how far this paper airplane can go, the process must be optimized in order to find the combination of these parameters that guarantees the best result, that is in which the paper airplane can go the furthest. Thus the DoE permits to determine how much each factor affect the system individually and as a group, in order to adjust them accordingly<sup>[19]</sup>.

### III.4 Defining Research Problem

Any researcher is ought to define their research objective prior to commencing any experimental or simulation work. In order to define a research problem properly, the objective must be clearly formulated, the research subject model chosen, and preliminary information analyzed.

To define a research objective or optimization subject, that is, the result or the value aimed to be maximized or minimized, it is necessary to verify if there exist interactions that change the quality of the research subject.

The next step is the choice of preliminary design of experiments. Herein a researcher must take into consideration all the singularities of the research problem and thus the chosen design would be used accordingly.

The next step is choice of research subject model, which is a plan for conducting the research whereas a theory is an outcome of research. Quantitative research, however, utilizes a model based on which the researcher proceeds their study.

### III.4.1 Factors

A factor is a quantity that is supposed to influence the system under study. It can be of two types (continuous or discrete):

A continuous factor can adopt all the real numerical values in its interval of variation, while a discrete factor can only take particular values included in a domain defined. These values are not necessarily numerical.

A factor is characterized by a range of variation, i.e. the set of all the values that this factor can take. This domain is habitually delimited by a lower bound (usually denoted by -1) and an upper bound (usually denoted by +1), and sometimes an intermediate bound is added (usually denoted by 0). These bounds represent the levels given to each variable. The more levels given for a variable, the more accuracy can be found in the results, yet this multiplies the necessary experimental work. The main point of using coded variables is acquiring information regarding factors effect without taking into consideration their real values.

Nevertheless, in case of utilizing the DoE as a modeling method, the experimenter would not be concerned with the economic costs of performing experimental work, thus, they can include as much levels as allowed by the available experimental data, considering that including more levels in the study would undoubtedly result in more accurate models.

### III.4.2 Experimental Domain

For a two-factor system, a continuous experimental domain can be illustrated (see Figure III.2) after having determined the levels, i.e. maximum and minimum values of each factor. Factor 1 varies between 10 and 40, while factor 2 varies between 15 and 50.

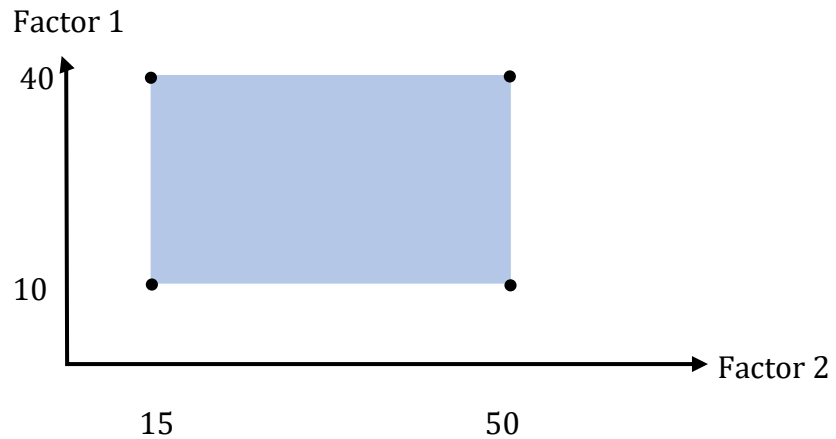


Figure III.2. Experimental Domain

An experimental domain represents all the points that can be included in the study. Any experimental point in this domain is defined by the value  $x_1$  of factor 1 and the value  $x_2$  of factor 2.

### III.4.3 Response

A response is an output quantity of interest to the experimenter, measured at each experiment to find the effect of factors on the system. The response can be qualitative or quantitative.

Mathematically, the response (aim function or optimization criterion) may have the form:

$$y = g(x_1, x_2, \dots, x_k)$$

where:

$y$  is the response, and  $x_1, x_2, \dots, x_k$  are controllable factors, changed during the experiment. This function can be approximated using a first order polynomial function (see equation III.1). Polynomials of other degrees can also be used and verified through statistical analysis thereafter.

Research solutions could be considered optimal if they are the maximum and minimum of the response function  $y$ . Yet another way of optimizing a response would be by adjusting the factors in order to find a certain response that is desired according to practical and operational requirements.

### III.5 Linear Regression Analysis

The modelling of relationships between a scalar response and one or more explanatory variables is called linear regression. If there is only one explanatory variable, it is called simple linear regression. The relationships are modeled using linear predictor functions whose unknown model parameters are estimated from the data.

A linear model can be presented by the equation:

$$y = a_0 + \sum_{i=1}^k a_i x_i + \sum_{\substack{i=1 \\ i \neq j}}^k a_{ij} x_i x_j \quad \text{III.1}$$

where:

$a_0$ ,  $a_i$ ,  $a_{ij}$  are polynomial coefficients or weights, relevant to the factors and their interactions. The degree of influence of the associated factors on the response can be estimated from the coefficient values. The higher the coefficient value of a factor, the higher its influence on the response. Linear regression analysis is followed by statistical analysis that aim to validate the model's coefficients.

### III.6 Full and Fractional Factorial Experiments

Principally in DoE, the desired response function is approximated by a polynomial, and regression coefficients are approximated based on experimental results. Accuracy and confidence of the obtained estimates for regression coefficients depend on the used design. Choice of the design has to do with determining the number of experimental points-trials and such a distribution of those points in a factorial space that facilitates obtaining the necessary information with a minimal number of design points-trials.

### III.6.1 Full Factorial Designs

It is one of the best-known statistical experimental designs, where all the possible experimental points, i.e. all possible combinations, are considered. This design offers a wider and more accurate information on the studied system.

If the number of factors is  $k$ , and the number of levels for every factor is  $p$ , then the number of experiments (also trials or design points)  $N$  allowing to test all the combinations would be:  $N=p^k$ , where the minimum number of levels is two.

### III.6.2 Fractional Factorial Designs

According to the ASQC (1983) Glossary & Tables for Statistical Quality Control, a fractional factorial design can be defined in the following way: *“A factorial experiment in which only an adequately chosen fraction of the treatment combinations required for the complete factorial experiment is selected to be run.”* There are several ways to choose which combinations will be included in the design, one of which is the Taguchi method, which will be used in chapter IV.

It should be mentioned that the accuracy as well as the cost of a fractional factorial design is decreased compared to a full fractional one. On the other hand, and since the number of levels is bound by the facility of performing experimental work, two-level factorial design are the most used in experimental research. Montgomery (1991) stated: *“It is our belief that the two-level factorial and fractional factorial designs should be the cornerstone of industrial experimentation for product and process development and improvement. He went on to say: There are, however, some situations in which it is necessary to include a factor (or a few factors) that have more than two levels”*<sup>[18]</sup>.

### III.6.3 Experimental Matrix

For any given phenomenon, there are factors and responses. By varying the factors, different responses are observed. In the following example, merely two factors,  $F_1$  and  $F_2$  will be considered. For each combination of factors  $(F_1, F_2) = (A_i, B_i)$ , a response  $Y_i$  is awaited, where  $i=1, 2, 3, 4$ .

By performing four experiments, four responses, Y1, Y2, Y3 and Y4 will be observed. The results are summarized in the following table:

Experiment Number	F1	F2	Y
1	A1	B1	Y1
2	A2	B2	Y2
3	A3	B3	Y3
4	A4	B4	Y4

Table III-1. Experimental matrix

Table III-1 is called the experimental matrix for the design in question. In the case of a response surface design, the factors are coded using the following formula:

$$x_i = \left[ \frac{u_i - (u_{\max} + u_{\min})}{2} \right] / \left[ \frac{u_{\max} - u_{\min}}{2} \right]$$

where:

$x_i$  is the value of the coded variable,

$u_i$  the initial value of the variable.

In constructing a DoE, and thus an experimental matrix, two essential aspects must be considered:

- **The Forbidden Tests:** it is important to specify the physical incompatibilities of associating levels between different factors. The construction of the design will have to take them into account so as not to create tests that are impossible to realize.
- **Mandatory Tests:** when a pre-study is being carried out, it is interesting to include in the design a few tests for which the results are known, combinations of essays encountered in the literature<sup>[16]</sup>.

### III.7 Conclusion

A strategy of experimentation that could address the challenges of time and resources is needed in modern scientific research.

This chapter has briefly presented the principle of Design of Experiments method as well as its advantages. The DoE is a whole field and cannot be addressed in a few pages of such manuscript. Nevertheless, the necessary notions for this work have been addressed, enabling the reader to be familiar with the DoE terms, as that would allow them to better understand the next chapter, in which the DoE will be applied on gas nitriding of a steel, and thus factorial designs and regression analysis will be explained in practice.



---

**Chapter Four**

**Modeling of Gas Nitriding by Design of  
Experiments**

---

## IV. Chapter Four: Modeling of Gas Nitriding of a Steel by Design of Experiments

### IV.1 Introduction

The Design of Experiments method is used to model the thermochemical surface treatment of gas nitriding applied to a low-alloy steel.

The objective of this study is to create a statistical model allowing to compare the effects of temperature, time and potential on the nitrided layer depth, in addition to creating a mathematical expression of the depth as function of these factors.

The model requires experimental results for the sake of establishing an statistical design with the minimum number of experiments in order to achieve the desired results while providing maximum precision.

### IV.2 Investigated Steel

The investigated steel was 35CrMo12, a structural steel for nitriding. This steel is widely used in the manufacture of shafts and gears due to its several advantageous properties, namely: wear and fatigue resistance, good hardenability with little distortion and good resistance to softening at high temperatures. The steel was austenitized at 900 °C for 0.5h and hardened by oil quenching and tempered at 600 °C for 1h<sup>[20]</sup>.

The chemical composition of this steel is given in Table IV-1.

C	Cr	Mo	Ni	V	Si	Mn
0.26	2.88	0.53	0.40	0.60	0.10-0.35	0.40-0.65

Table IV-1. Chemical composition (in wt %) of the steel investigated<sup>[20]</sup>

Using the materials property simulation software JMatPro, the TTT and CTT diagrams of this steel are given in Figure IV.1 and Figure IV.2, respectively.

TTT

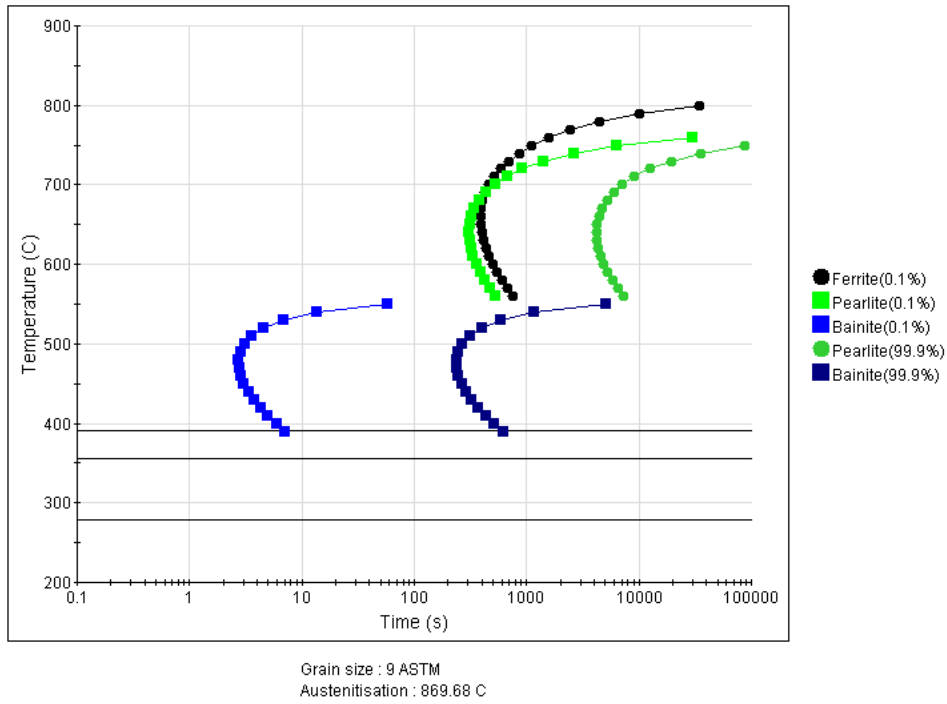


Figure IV.1. TTT diagram for 35CrMo12, simulated with JMatPro

CCT

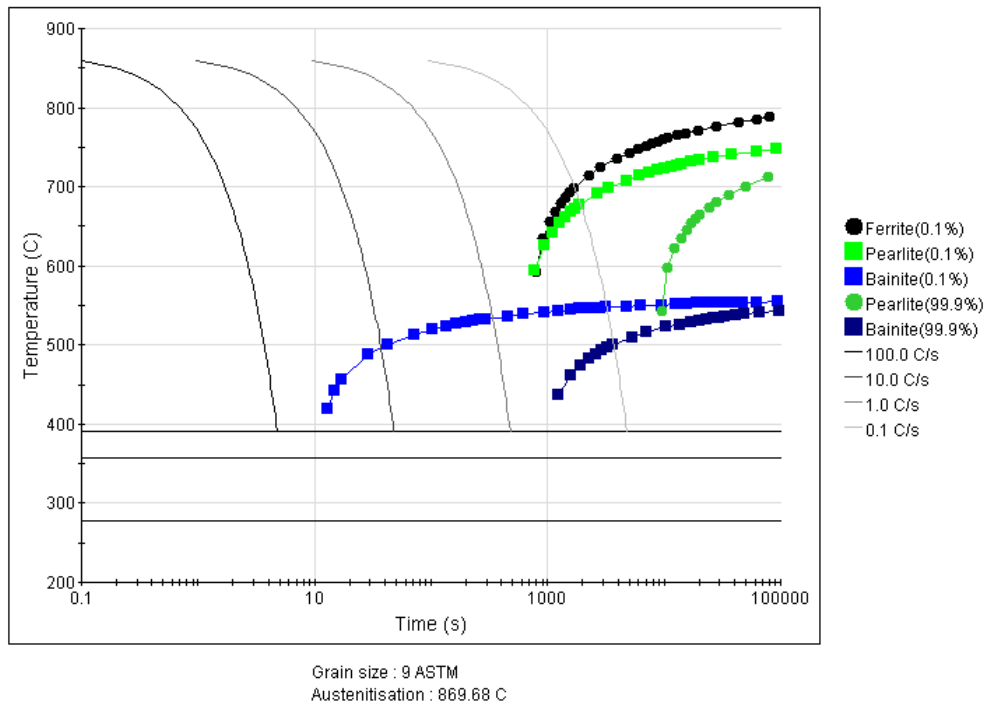


Figure IV.2. CCT diagram for 35CrMo12, simulated with JMatPro

### IV.3 Defining Research Problem

Defining research problem is vital for the completion of this study. This means choosing the response to be studied and optimized as well as the factors whereon this response is dependent and whose influence must be determined.

#### IV.3.1 Responses

The gas nitriding treatment principally consists of diffusing nitrogen into the surface of a material. Hence, the choice of responses in this treatment should serve in calculating the amount of nitrogen that was added. To this end, the nitrided layer (NL) depth, which is the furthestmost distance that the diffused nitrogen can reach within the material, is the chosen response of this system.

#### IV.3.2 Factors

The factors chosen for this simulation are preliminary determined to have the greater influence on the response: nitrided layer depth. These factors are the following nitriding temperature, nitriding time and nitriding potential. The effect of other factors, such as pressure, will be neglected in this study, while

For each factor, the chosen three values (levels): upper value, intermediate value and lower value, are presented as follows:

Factor	Temperature (°C)	Time (hours)	Potential
Level -1	470	24	10
Level 0	520	48	30
Level +1	570	72	80

**Table IV-2. Factors levels**

As shown in Table IV-2, the upper, intermediate and lower values are coded -1, 0, and 1, respectively. These levels were chosen according to the experimental data of gas nitriding of the steel 35CrMo12, performed by Shahjahan Mridha in 2007<sup>[20]</sup>.

Equations IV.1, IV.2 and IV.3 will be used to switch between variables in real units and variables given in coded units:

$$x_1 = \frac{T - T_0}{\Delta T} \quad \text{IV.1}$$

$$x_2 = \frac{t - t_0}{\Delta t} \quad \text{IV.2}$$

where:  $T_0$  and  $t_0$  and the intermediate values for the temperature and time, respectively, and:

$$\Delta T = T_0 - T_1 = T_2 - T_0$$

$$\Delta t = t_0 - t_1 = t_2 - t_0$$

For the nitriding potential, the intermediate value is not in the center of interval, that is to say, it does not satisfy the relationship:

$$\Delta K_n = K_{n0} - K_{n1} = K_{n2} - K_{n0}$$

Therefore, it is necessary to consider that:

$$K_{n0} = \frac{(K_{n1} + K_{n2})}{2} \text{ and } \Delta K_n = \frac{(K_{n2} - K_{n1})}{2}, \text{ thus:}$$

$$x_3 = \frac{K_n - \frac{(K_{n1} + K_{n2})}{2}}{\frac{(K_{n2} - K_{n1})}{2}} \quad \text{IV.3}$$

### IV.3.3 Experimental Domain

The experimental domain of a three factors system could be represented by a cube. Since the chosen variables are of three levels each, there are 27 possible combinations. Thus, 27 experimental points, as depicted in Figure IV.3.

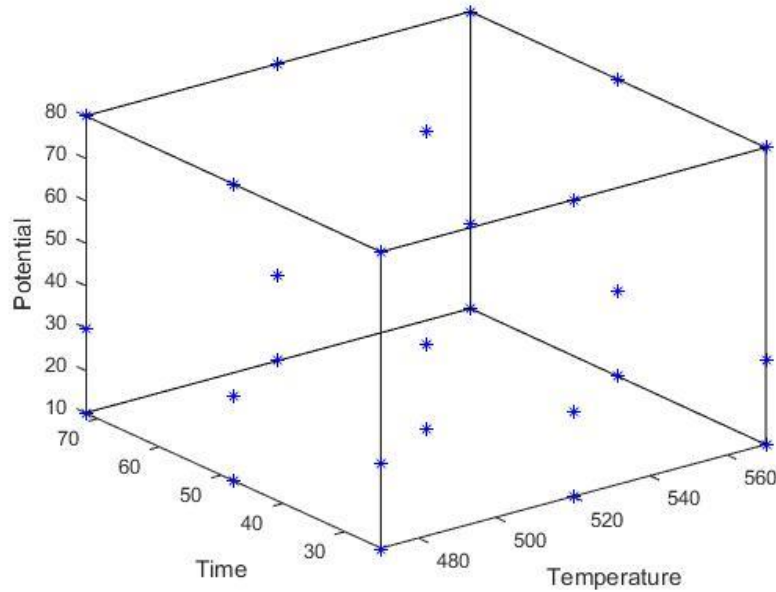


Figure IV.3. Experimental domain

After having established a mathematical formula, every point (T, t, K<sub>n</sub>) inside this cube can be considered for calculating the NL depth.

#### IV.4 Mathematical Model

The chosen model was that of a full factorial design of three factors and three levels, 3<sup>3</sup>, with a first order polynomial. The linear regression expression of the response is given as follows:

$$y = a + a_1x_1 + a_2x_2 + a_3x_3 + a_{12}x_1 \cdot x_2 + a_{13}x_1 \cdot x_3 + a_{23}x_2 \cdot x_3 + a_{123}x_1 \cdot x_2 \cdot x_3 \quad \text{IV.4}$$

where:

y is the measured response of the system,

a is the intercept, a constant of the system,

x<sub>1</sub>, x<sub>2</sub> and x<sub>3</sub> are the levels of temperature, time, and potential, respectively.

a<sub>1</sub>, a<sub>2</sub> and a<sub>3</sub> are coefficients or weights relevant to temperature, time and potential, respectively,

a<sub>12</sub> is the coefficient or weight relevant to the interaction between temperature and time,

a<sub>13</sub> between temperature and potential, a<sub>23</sub> between time and potential, and a<sub>123</sub> between

all the three factors.

As a matter of fact, this equation could be of second order, or even third order, by including other terms, such as  $x_1^2$ ,  $x_2^2$ ,  $x_1^3$ , etc. Yet, for the sake of simplicity, a first order polynomial is used.

### IV.5 Factorial Designs

As mentioned in chapter 3, there are two types of factorial designs: full factorial designs and fractional factorial designs. The choice of the convenient design is bound by the facility of performing experimental work by means of cost, time, etc., in case of using the DoE to rationalize an experience, and by the availability of experimental data, in case of using the DoE in modeling of a given phenomenon. Hence, modeling with DoE requires experimental data for gas nitriding of the investigated steel. Since this model is of one response, the needed results are in the form:  $(T_i, t_i, K_{n_i}) \rightarrow d$ , where  $i, j=1,2,3$ .

#### IV.5.1 Full Factorial Design

To perform a full factorial analysis of a three factors, three levels system, the experimental results of 27 different experiences are required. This design fulfills all the possible combinations of such system.

The experimental matrix of a  $3^3$  full factorial design relevant to the system of equation IV.4 wherein the lower, intermediate and upper levels are coded -1, 0 and 1, respectively, takes the following form:

$$X = \begin{bmatrix} 1 & -1 & -1 & -1 & 1 & 1 & 1 & -1 \\ 1 & -1 & -1 & 0 & 1 & 0 & 0 & 0 \\ 1 & -1 & -1 & 1 & 1 & -1 & -1 & 1 \\ 1 & -1 & 0 & -1 & 0 & 1 & 0 & 0 \\ 1 & -1 & 0 & 0 & 0 & 0 & 0 & 0 \\ 1 & -1 & 0 & 1 & 0 & -1 & 0 & 0 \\ 1 & -1 & 1 & -1 & -1 & 1 & -1 & 1 \\ 1 & -1 & 1 & 0 & -1 & 0 & 0 & 0 \\ 1 & -1 & 1 & 1 & -1 & -1 & 1 & -1 \\ 1 & 0 & -1 & -1 & 0 & 0 & 1 & 0 \\ 1 & 0 & -1 & 0 & 0 & 0 & 0 & 0 \\ 1 & 0 & -1 & 1 & 0 & 0 & -1 & 0 \\ 1 & 0 & 0 & -1 & 0 & 0 & 0 & 0 \\ 1 & 0 & 0 & 0 & 0 & 0 & 0 & 0 \\ 1 & 0 & 0 & 1 & 0 & 0 & 0 & 0 \\ 1 & 0 & 1 & -1 & 0 & 0 & -1 & 0 \\ 1 & 0 & 1 & 0 & 0 & 0 & 0 & 0 \\ 1 & 0 & 1 & 1 & 0 & 0 & 1 & 0 \\ 1 & 1 & -1 & -1 & -1 & -1 & 1 & 1 \\ 1 & 1 & -1 & 0 & -1 & 0 & 0 & 0 \\ 1 & 1 & -1 & 1 & -1 & 1 & -1 & -1 \\ 1 & 1 & 0 & -1 & 0 & -1 & 0 & 0 \\ 1 & 1 & 0 & 0 & 0 & 0 & 0 & 0 \\ 1 & 1 & 0 & 1 & 0 & 1 & 0 & 0 \\ 1 & 1 & 1 & -1 & 1 & -1 & -1 & -1 \\ 1 & 1 & 1 & 0 & 1 & 0 & 0 & 0 \\ 1 & 1 & 1 & 1 & 1 & 1 & 1 & 1 \end{bmatrix}$$

The matrix X is compiled of 6 columns (as coefficients of the model) and 27 lines (as experiences).



Experience N°	Temperature (°C)	Time (hours)	Potential	NL Depth (µm)
1	470	24	10	70.71067812
2	470	24	30	118.3215957
3	470	24	80	141.4213562
4	470	48	10	92.19544457
5	470	48	30	184.3908891
6	470	48	80	212.1320344
7	470	72	10	122.4744871
8	470	72	30	242.899156
9	470	72	80	273.8612788
10	520	24	10	126.4911064
11	520	24	30	118.3215957
12	520	24	80	212.1320344
13	520	48	10	148.3239697
14	520	48	30	275.680975
15	520	48	80	296.6479395
16	520	72	10	183.0300522
17	520	72	30	330.1514804
18	520	72	80	374.1657387
19	570	24	10	187.0828693
20	570	24	30	356.3705936
21	570	24	80	391.1521443
22	570	48	10	252.9822128
23	570	48	30	438.178046
24	570	48	80	553.1726674
25	570	72	10	363.3180425
26	570	72	30	547.7225575
27	570	72	80	655.7438524

Table IV-3 Experimental matrix for the 3<sup>3</sup> full factorial design relevant to gas nitriding of the steel 35CrMo12<sup>[20]</sup>

Following the method of linear regression, the coefficients are calculated by the formula IV.5 and presented in Table IV-4.

$$\hat{a} = (X^t \cdot X)^{-1} \cdot X^t \cdot \hat{y} \quad \text{IV.5}$$

Coefficient	Value
a	269.2249925
a <sub>1</sub>	127.0731148
a <sub>2</sub>	76.1868151
a <sub>3</sub>	86.87889907
a <sub>12</sub>	26.9497961
a <sub>13</sub>	37.88762334
a <sub>23</sub>	22.87728392
a <sub>123</sub>	0.960052684

Table IV-4. Coefficients of the 3<sup>3</sup> full factorial model relevant to gas nitriding of the steel 35CrMo12

The predicted NL depths, via the established full factorial model, are given as follows:

Real NL depth (experimental)( $\mu\text{m}$ )	Predicted NL depth (model) ( $\mu\text{m}$ )	Residual (in absolute value)
70.71067812	65.84081424	4.869863878
118.3215957	92.91485874	25.40673692
141.4213562	119.9889032	21.432453
92.19544457	93.16060201	0.965157433
184.3908891	142.1518777	42.23901141
212.1320344	191.1431535	20.98888088
122.4744871	120.4803898	1.994097367
242.899156	191.3888967	51.51025929
273.8612788	262.2974037	11.56387504
126.4911064	129.0365623	2.545455853
118.3215957	193.0381774	74.71658175
212.1320344	257.0397926	44.90775821
148.3239697	182.3460934	34.0221237
275.680975	269.2249925	6.455982527
296.6479395	356.1038916	59.4559521
183.0300522	235.6556246	52.62557245
330.1514804	345.4118076	15.26032723
374.1657387	455.1679906	81.00225193
187.0828693	192.2323103	5.14944094
356.3705936	293.1614961	63.20909754
391.1521443	394.0906819	2.938537572
252.9822128	271.5315849	18.54937207
438.178046	396.2981073	41.87993871
553.1726674	521.0646297	32.10803774
363.3180425	350.8308595	12.487183
547.7225575	499.4347185	48.28783901
655.7438524	648.0385775	7.705274927

**Table IV-5. Comparison between the experimental NL depths and the ones predicted by the full factorial model**

Calculating the residual  $r$  allows for estimating the accuracy of the model:

$$r = |d_m - d_p|$$

where:

$d_m$  is the measured (experimental) NL depth,

$d_p$  is the predicted NL depth.

Figure IV.4 depicts a comparison between the variation of values of NL depth given by the full factorial model and those of experimental data. It is clear that full factorial model values vary in the same way as the experimental ones.

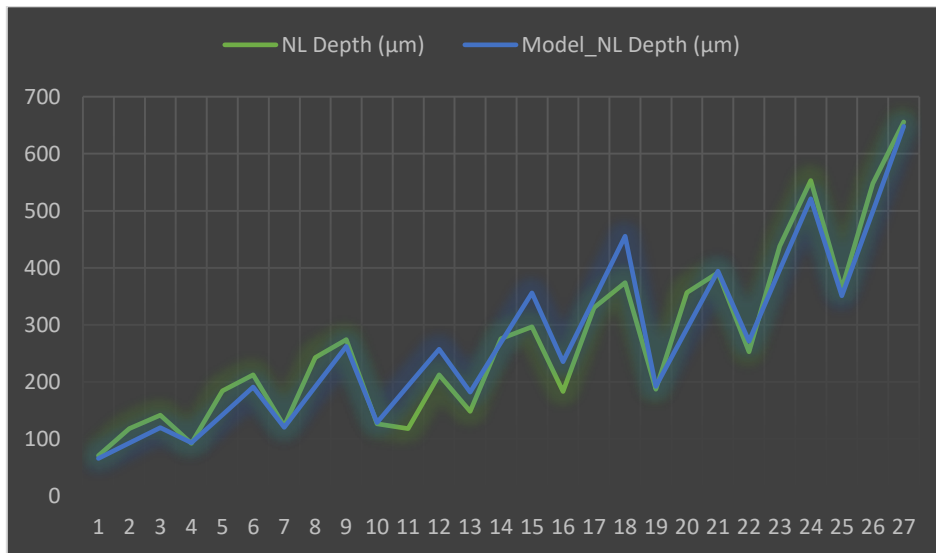


**Figure IV.4. Comparing the full factorial model to experimental data**

### IV.5.2 Fractional Factorial Design

For a fractional factorial design, only 9 experiences are required, according to the tables of Taguchi. These tables give the appropriate combinations for a  $3^3$  fractional designs, thus it is not necessary to perform all the combinations. This design follows the principle: for each level of a particular parameter, all  $L$  levels of each of the  $(P-1)$  other parameters are tested at least once.

Taguchi, $P = 3, L = 3$				
Run #	$a$	$b$	$c$	$X$
1	1	1	1	$X_1$
2	1	2	2	$X_2$
3	1	3	3	$X_3$
4	2	1	2	$X_4$
5	2	2	3	$X_5$
6	2	3	1	$X_6$
7	3	1	3	$X_7$
8	3	2	1	$X_8$
9	3	3	2	$X_9$

Table IV-6. Taguchi combinations for the fractional factorial  $3^3$  design<sup>[21]</sup>

The variables can be coded 1, 2 and 3, or -1, 0 and +1, there is no difference. The experimental matrix of a  $3^3$  fractional factorial design, according to Taguchi arrays, relevant to the system of equation IV.4 wherein the lower, intermediate and upper levels are coded -1, 0 and 1, respectively, takes the following form:

$$Y = \begin{bmatrix} 1 & -1 & -1 & -1 & 1 & 1 & 1 & -1 \\ 1 & -1 & 0 & 0 & 0 & 0 & 0 & 0 \\ 1 & -1 & 1 & 1 & -1 & -1 & 1 & -1 \\ 1 & 0 & -1 & -1 & 0 & 0 & 0 & 0 \\ 1 & 0 & 0 & 0 & 0 & 0 & 0 & 0 \\ 1 & 0 & 1 & 1 & 0 & 0 & -1 & 0 \\ 1 & 1 & -1 & 1 & -1 & 1 & -1 & -1 \\ 1 & 1 & 0 & -1 & 0 & -1 & 0 & 0 \\ 1 & 1 & 1 & 0 & 1 & 0 & 0 & 0 \end{bmatrix}$$

Experience N°	Temperature (°C)	Time (hours)	Potential	NL Depth (µm)
1	470	24	10	70.71067812
2	470	48	30	184.3908891
3	470	72	80	273.8612788
4	520	24	30	118.3215957
5	520	48	80	296.6479395
6	520	72	10	183.0300522
7	570	24	80	391.1521443
8	570	48	10	252.9822128
9	570	72	30	547.7225575

Table IV-7. Experimental matrix for the Taguchi 3<sup>3</sup> fractional factorial design relevant to gas nitriding of the steel 35CrMo12<sup>[20]</sup>

Likewise, following the method of linear regression, the coefficients obtained are as follows:

Coefficient	Value
a	257.6465942
a <sub>1</sub>	144.5109836
a <sub>2</sub>	111.2522083
a <sub>3</sub>	82.18383353
a <sub>12</sub>	12.72152725
a <sub>13</sub>	81.02792655
a <sub>23</sub>	68.05727759
a <sub>123</sub>	0

Table IV-8. Coefficients of the Taguchi 3<sup>3</sup> fractional factorial model relevant to gas nitriding of the steel 35CrMo12

It is noticed that this model does not give any value for the a<sub>123</sub> coefficient, which comes in accordance with the full factorial model, wherein the value of the a<sub>123</sub> coefficient was very small.

The predicted NL depths, via the established fractional factorial model, are given as follows:

Real NL depth (experimental)( $\mu\text{m}$ )	Predicted NL depth (model) ( $\mu\text{m}$ )	Residual (in absolute value)
70.71067812	81.50630019	10.79562207
184.3908891	113.1356107	71.25527849
273.8612788	280.8794763	7.018197556
118.3215957	146.3943859	28.07279022
296.6479395	339.8304278	43.18248827
183.0300522	218.6576914	35.62763925
391.1521443	373.3383247	17.81381962
252.9822128	238.9458177	14.03639511
547.7225575	526.1313134	21.59124413

**Table IV-9. Comparison between the experimental NL depths and the ones predicted by the fractional factorial model**

Figure IV.5 shows a comparison between the variation of values of NL depth given by the fractional factorial model and those of experimental data. Again, fractional model values vary in the same way as the experimental ones.

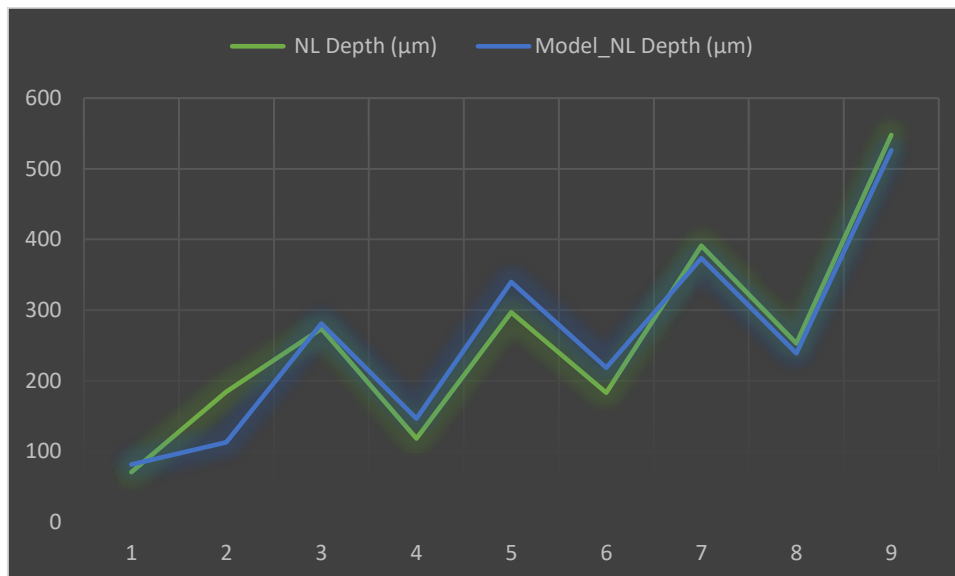


**Figure IV.5. Comparing the fractional factorial model to experimental data**

### IV.5.3 Comparing the two Models

The best way to investigate the accuracy of the two factorial models is by running a statistical comparison via the standard errors of the two models. The standard error permits the researcher to construct confidence intervals about the obtained sample statistic.

The standard error SE is given by the following formula:

$$SE = \frac{SD}{\sqrt{N}}$$

where:

N is the number of experiences,

SD is the standard deviation given by the formula:

$$SD = \sqrt{\frac{\sum_{i=1}^N (d_i - \bar{d})^2}{N - 1}}$$

where d is the NL depth.

For the full factorial model, the standard error is: 44.57714047

For the fractional factorial model, the standard error is: 71.22424857

Since the standard error of the fractional model is higher than that of the full factorial one, it is fair to state that the full factorial model is more accurate. Consequently, solely the full factorial model will be considered in the upcoming analysis. The equation of the model giving the NL depth as function of system coded variables, and taking into account their interactions, is the following:

$$\begin{aligned} d = & 269.2249925 + (127.0731148)x_1 + (76.1868151)x_2 + (86.87889907)x_3 \\ & + (26.9497961)x_1 \cdot x_2 + (37.88762334)x_1 \cdot x_3 \\ & + (22.87728392)x_2 \cdot x_3 + (0.960052684)x_1 \cdot x_2 \cdot x_3 \end{aligned} \quad \text{IV.6}$$

In order to find the model equation with real values instead of coded ones, i.e. as function of temperature, time and potential, the equations IV.1, IV.2 and IV.3 are replaced in IV.6. Therefore, the model is transposed into the real system, to obtain the equation giving the nitrated layer depth as function of nitriding temperature, time and potential, in the case of the steel 35CrMo12.



$$d(T, t, K_n) = \frac{(240013171)TtK_n}{10500000000000} + \frac{(671496667)tK_n}{43750000000} + \frac{(8991879493)TK_n}{43750000000} + \frac{(11250506159)Tt}{52500000000} \quad \text{IV.7}$$

$$+ \frac{(47126749113)T}{87500000000} - \frac{(643613364349)t}{70000000000} - \frac{(832344639197)K_n}{87500000000} - \frac{3781580520177}{17500000000}$$

where: Temperature T is in °C, time t is in hours, and NL depth d is in μm.

## IV.6 Statistical Analysis

The implementation of statistical tests is necessary for judging the quality of the obtained model by means of describing the variations of the chosen response according to the variations of the factors.

The statistical analysis of the model is based on testing the null hypothesis ( $H_0$ ) that says that the model allows not for describing the variation of the test results.

This law is used to find from which particular value, called the critical value, the numerator of the quantity F is significantly greater than the denominator. In other words, F tells us about the probability Prob F of rejecting the null hypothesis. Therefore, the smallest value of this probability is required. If Prob F is below 5%, there is no reason to reject the model<sup>[22]</sup>.

This step of the statistical analysis leads to the construction of the regression analysis table and the determination of the descriptive quality of the model. The regression analysis consists of explaining the total variation of the response defined from the sum of the squares of the differences between the test results and their mean. The following analysis will consider the full factorial model.

- **Total Sum of Squares:** it measures how far individual measurements are from the mean:

$$TSS = SSR + RSS = \sum_{i=1}^{27} (d_i - \bar{d})^2$$

where:

$d_i$  are the measured responses,

$\bar{d}$  is the arithmetic mean of the measured responses.

The term SSR (Sum of Squares due to Regression) reflects the variation of the calculated responses around their mean:

$$SSR = \sum_{i=1}^{27} (\widehat{d}_i - \bar{d})^2$$

$\widehat{d}_i$  are the responses calculated by the model.

The term RSS (Residual Sum of squares) is a measure of the discrepancy between the experimental data and the model:

$$RSS = \sum_{i=1}^{27} (d_i - \widehat{d}_i)^2$$

- **F Distribution:** it is used to test for equality of variances. The Fisher-Snedecor F test will make it possible to decide whether the equation of the model does indeed establish a relationship between the variation of the factors and the response.

$$F = \frac{SSR/\text{dof}_{SSR}}{RSS/\text{dof}_{RSS}} = \frac{SSR/(p-1)}{RSS/(N-p)}$$

where:

dof: number of degrees of freedom,

p - 1 is the degree of freedom relevant to SSR,

p is the number of terms in the model equation,

N - 1 is the degree of freedom relevant to RSS,

N is the number of experiences performed.

The various regression calculations leading to the calculation of the F probability are reported in Table IV-10, as follows:

Source	Sum of Squares	dof	F	Prob F
Regression (Model)	SSR=563228.0843	p-1=7	40.49131209	4.1977.10 <sup>-10</sup>
Residual	RSS=37755.3076	N-p=19		
Total	TSS=600983.3919	N-1=26		

**Table IV-10. Results of linear regression analysis**

The value of Prob F is negligible. Therefore, there is no reason to reject the model.

- **Correlation coefficient  $R^2$ :** determining the value of the linear multiple correlation coefficient  $R^2$  is a complementary analysis that allows for further verifying the quality of the model. This coefficient is defined as the fraction of variations in the response explained by the model alone.

$$R^2 = \frac{SSR}{RSS}$$

$R^2$  takes values between -1 and +1. The values -1 and +1 signify that there is an exact linear relationship for the variations of the model response.

For the full factorial model,  $R^2=0.968079259$  shows that 96.8% of the variations in responses are explained by the model in the chosen experimental domain.

It should be noted that it is possible to neglect the coefficient  $a_{123}$  and eliminate it from the equation, for there is a strong possibility that it is equal to 0. This probability is based on calculating the quantity:

$$t_{obs} = \frac{|a_i|}{S_r \sqrt{c_{ii}}}$$

where  $S_r = \sqrt{\sigma_r^2}$  is the standard residual deviation,  $\sigma_r^2 = \frac{RSS}{N-p}$  (residual variance), and  $c_{ii}$  is a variation coefficient corresponding to the diagonal term of rank  $i$  of the dispersion matrix noted  $(X^t X)^{-1}$  in the least squares method.

This distribution function, then, is used to find from which particular value, called the critical value, the numerator of the quantity  $t_{obs}$  is significantly different from 0 for a probability  $\alpha$ <sup>[22]</sup>.

The results of all the coefficients are as follows:

Coefficient	Probability p
a <sub>1</sub>	2.27005E-10
a <sub>2</sub>	6.98816E-07
a <sub>3</sub>	1.02246E-07
a <sub>12</sub>	0.049876333
a <sub>13</sub>	0.008326679
a <sub>23</sub>	0.091446522
a <sub>123</sub>	0.952062707

**Table IV-11. Statistical test results for the full factorial model coefficients**

Nevertheless, although the probability value of the coefficient a<sub>123</sub> is high, it can be kept in the equation, as it will not affect the accuracy of the upcoming results. All the remaining coefficients have a small probability of being equal to 0.

All the calculations were executed using the linear regression tool on Microsoft Excel 2016.

### **IV.7 Study of Factors Effects on the Nitrided Layer Depth**

The construction of the average effects plot uses the values of the coefficients of the predictive model of coded values with a bar graph. The length of each bar is proportional to the value of the effect of this factor on the evolution of the NL depth.

- **In case of full factorial design**

Figure IV.6 shows the factors influencing the evolution of the nitrided layer in case of full factorial design. It is apparent that the nitriding temperature is given a slightly more important effect than the other two factors, followed by the nitriding potential, and then the nitriding time.

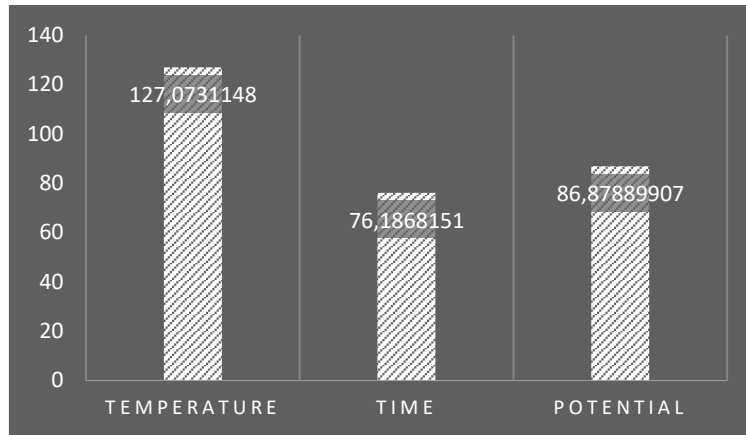


Figure IV.6. Effects of factors on the NL depth in case of full factorial design

- **In case of fractional factorial design**

Figure IV.7 shows the factors influencing the evolution of the nitrated layer in case of fractional factorial design. The nitriding temperature still has the highest effect, yet herein it is followed by nitriding time, and then the nitriding potential.

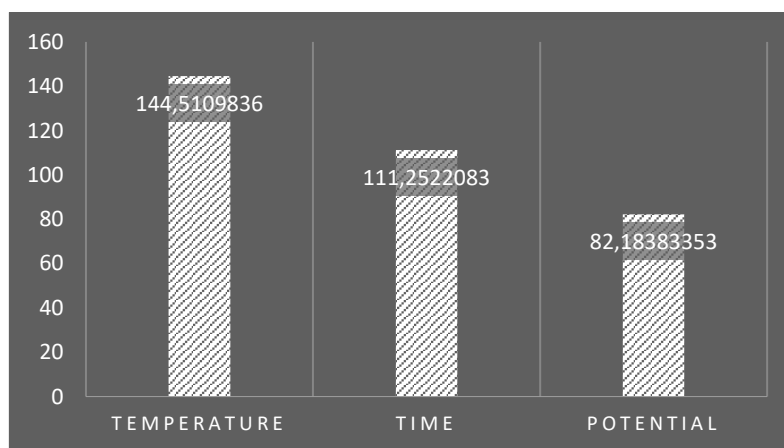


Figure IV.7. Effects of factors on the NL depth in case of fractional factorial design

It is noted that the factors effect provided by the two models differ, not only in value, but also, and most importantly in order of influence, as the fractional factorial design gives time the second order of influence, then comes potential, while potential comes second before time in the full factorial design. Yet still, temperature remains the most influencing factor in both designs. Metallurgically, the reason for which temperature is the most influencing factor on the diffusion of nitrogen is because of the nature of diffusion itself, as it is a thermally active phenomenon.

Overall, it has been settled that the full factorial design gives better results. Therefore, this difference can eventually be ascribed to the better accuracy of the full factorial design, and thus this result would be considered and given more importance.

### IV.8 Testing the Model Using Experimental Examples

Often the validation of a model seems to consist of nothing more than quoting the R<sup>2</sup> statistic (which measures the fraction of the total variability in the response that is accounted for by the model). Therefore, the obtained equation IV.7 should provide valuable results of NL depth, considering that it has passed the previous statistical tests. Nevertheless, the model can be further tested using examples from experimental results of gas nitriding of the steel 35CrMo12.

Considering a gas nitriding treatment of the steel 35CrMo12 performed under the following conditions:

Nitriding temperature: 570 °C

Nitriding time: 96 hours

Nitriding potential: 80

Using the model, the calculated NL depth is: 746,86 μm.

According to the study of Mridha in 2007, the obtained NL depth under the same conditions is approximately 788,66μm<sup>[20]</sup>. This shows that the obtained mathematical formula is valid in calculating approximate values of the NL depth for the steel 35CrMo12.

### IV.9 Graphical Representation of NL Depth Function

The function  $d=f(T, t, K_n)$  has three variables:

$$d(T, t, K_n) = \frac{(240013171)TtK_n}{1050000000000} + \frac{(671496667)tK_n}{43750000000} + \frac{(8991879493)TK_n}{43750000000} + \frac{(11250506159)Tt}{52500000000} + \frac{(47126749113)T}{87500000000} - \frac{(643613364349)t}{70000000000} - \frac{(832344639197)K_n}{87500000000} - \frac{3781580520177}{17500000000} \quad \text{IV.8}$$

where:  $470 < T$  (°C)  $< 570$

$10 < t$  (hours)  $< 120$

$1 < K_n < 99$

While it is not possible to plot such function in space, giving a certain value to each variable and varying the remaining two, every time, would provide an idea on how the NL depth develops as function of its parameters.

Every variable was kept at three levels. The chosen levels were the same ones considered in the factorial designs (see Table IV-2).

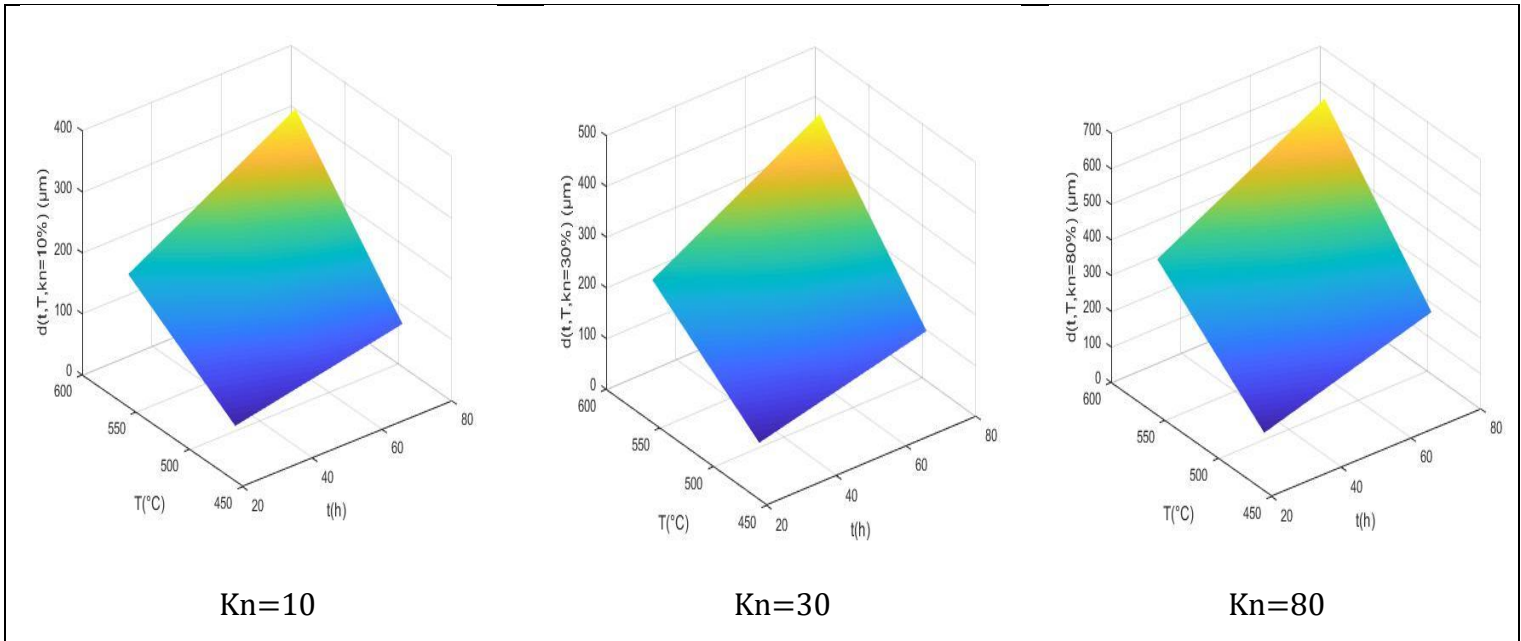


Figure IV.8. NL depth plot at fixed values of potential

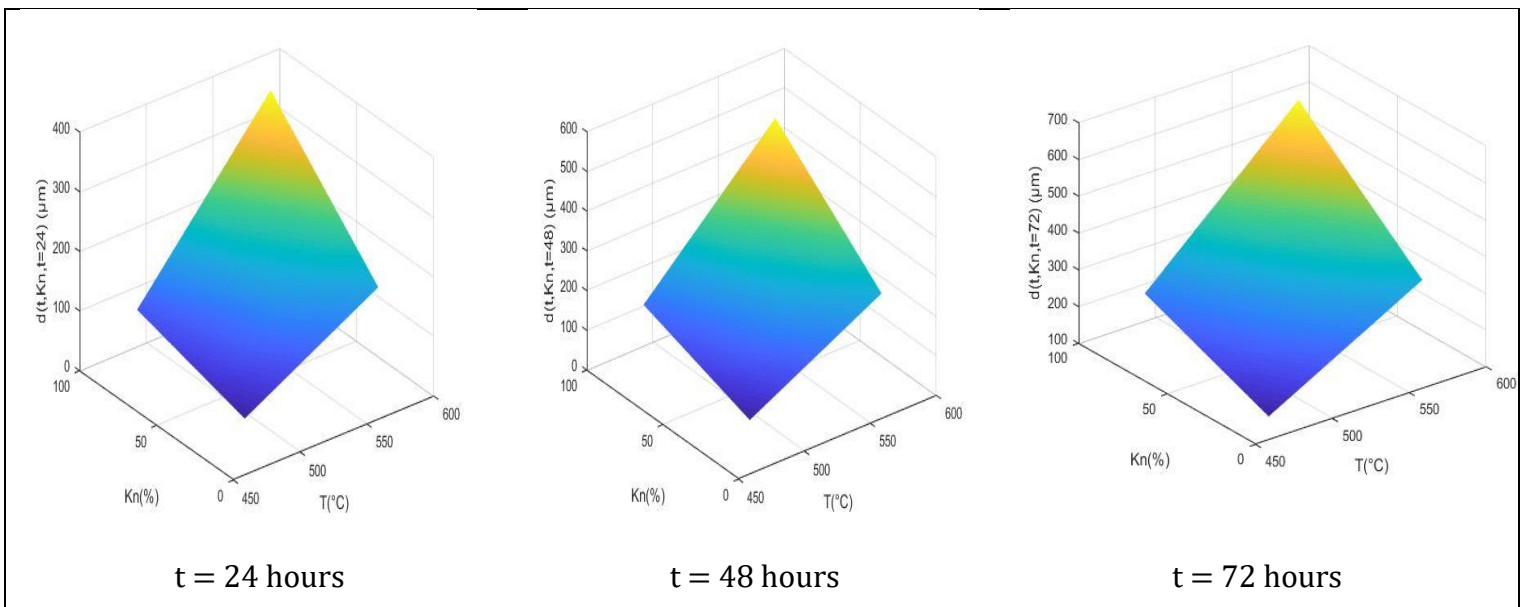


Figure IV.9. NL depth plot at fixed values of time

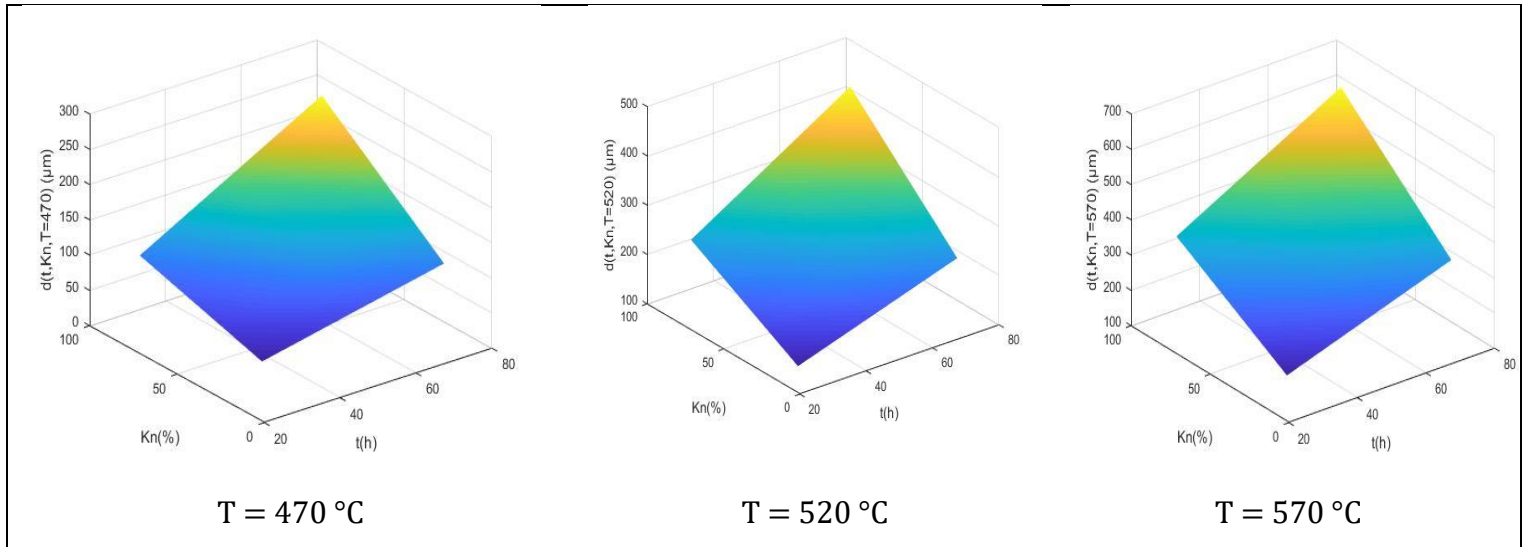


Figure IV.10. NL depth plot at fixed values of temperature

It should be noted that these graphs were plotted in Matlab R2017.

Table IV-12 gives the minimum and maximum values of the NL depth according to all the three levels of each factor. These value further confirms the effect of each factor on the NL depth.

Graph	max	min
Kn=10	350	65
Kn=30	435	81
Kn=80	648	120
T=470	262	66
T=520	455	129
T=570	648	192
t=24	394	66
t=48	521	93
t=72	648	120

Table IV-12. Minimum and maximum values of NL depth function

In order to better understand the development of the NL depth function, its variations as function of time were plotted by fixing the two other variables at different values, see



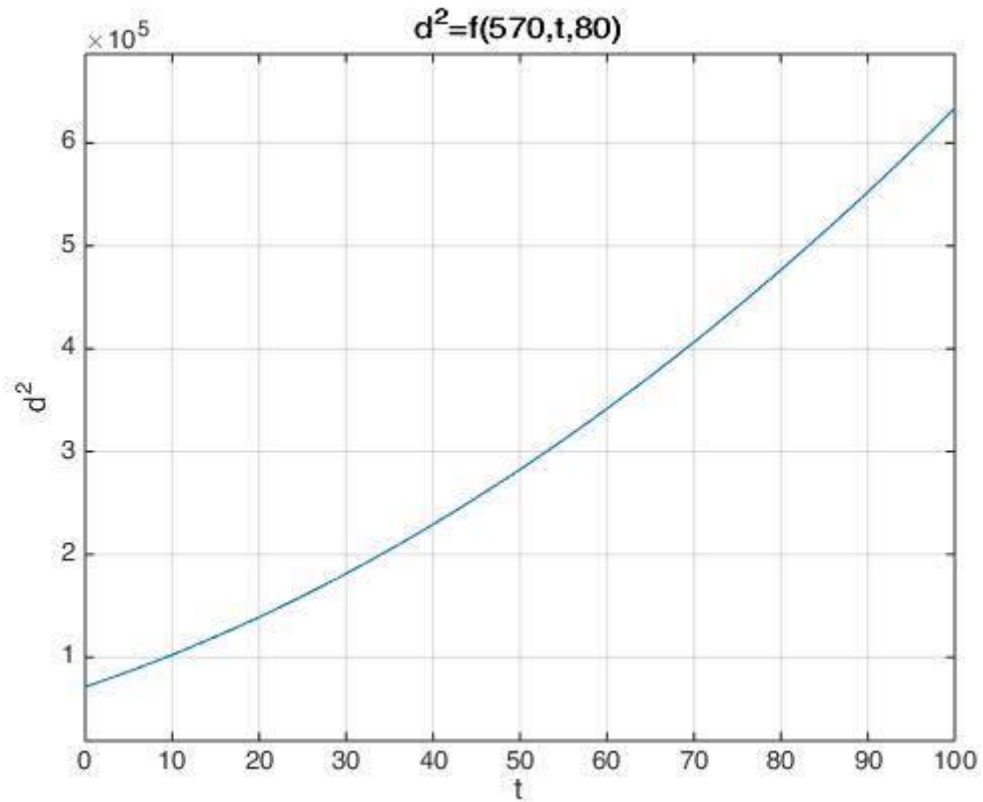


Figure IV.11. NL depth as function of time

This shows that the NL depth increases parabolically with the increase of nitriding time, which is in accordance with Mridha 2007<sup>[20]</sup>.

## IV.10 Conclusion

In this chapter, the DoE was employed for two objectives: a comparative study wherein the effects of the nitriding temperature, time and potential on the NL depth have been compared, and a regression model, wherein a polynomial function giving the NL depth as function of the three previous factors has been established.

It was found that the nitriding temperature has the greatest influence on the NL depth, followed by potential, and then time. The interactions between factors is also found to have a considerable effect on the response.

The established NL depth function has been successfully validated through statistical analysis, and it varies in the same way as the experimental data of gas nitriding of the steel 35CrMo12. This function can be used for several optimization purposes, especially optimizing the response, the NL depth, which will be addressed in the following chapter.

---

**Chapter Five**  
**Optimizing a Response Using the DoE**  
**Model**

---

## V. Chapter Five: Optimizing a Response Using the DoE Model

### V.1 Introduction

Among the most common uses of Design of Experiments is optimizing a response, which could be the most needed as well as the hardest research problem in various engineering fields. Whether it is a ratio, a percentage, or a numerical value, optimization remains one of the most essential scientific research endeavors.

This chapter is an exploitation of the DoE mathematical model established in chapter IV.

### V.2 Definition

Optimization can be defined as the process of finding the greatest, least or a specific value of a function taking into consideration some constraints. This value should have a significant technical importance with regards to a given field.

In this work, a polynomial function giving the NL depth as function of nitriding temperature, time and potential has been established. Hence, this function would facilitate the optimization process.

### V.3 Optimizing the Nitrided Layer Depth

The chosen response in the established DoE model is the NL depth, which can be defined as the distance whereby nitrogen is diffused into the material.

As aforementioned, optimization consists of finding the greatest, least, or any desirable value of a certain function. In gas nitriding of steel, it might seem that the goal is to maximize the NL depth, since nitrogen is the responsible of hardening the nitrided part along with other improvements in properties, however, NL depths higher than 600 $\mu\text{m}$  are somewhat undesirable, for they increase porosity, weaken the surface layer, and cause the percentage of  $\epsilon$  structure to be greater than that of  $\gamma'$  structure, resulting in an increase of residual stresses, which would necessitate an annealing treatment to rectify these changings, and that is undesirable for economic reasons. Overall, NL depths higher than 600 $\mu\text{m}$ , even of 800 $\mu\text{m}$  or 100 $\mu\text{m}$ , would not bring better properties than those of 600 $\mu\text{m}$ <sup>[10]</sup>. Therefore, the best NL depth for industrial applications is that of 600 $\mu\text{m}$ .

Utilizing the expression IV.7 to optimize the NL depth for 600 $\mu\text{m}$  consists of finding the combination of nitriding temperature, time and potential allowing to find  $d=600\mu\text{m}$ . Thus, a simple optimization algorithm was created for this purpose.

### V.3.1 Optimization Algorithm

Since solving a three variables equation is impossible, the algorithm has two loops: in the first one the values of time are varied, and in the second one the values of potential are varied, and at last, when both time and potential have a given value, the program solves an equation of one unknown, temperature.

The algorithm works as follows:

#### Step 1: Define the coefficients of the equation

The coefficients of the equation IV.7 are defined as a, b, c, d, e, f, g, h and j, as well as the NL depth d.

The equation is in the form:

$$d = a.T.t.k + b.t.k + c.T.k + d.T.t + f.T + g.t + h.k + j$$

and:

$$a = (240013171 / 10500000000000)$$

$$b = (671496667 / 43750000000)$$

$$c = (8991879493 / 437500000000)$$

$$d = (11250506159 / 525000000000)$$

$$f = (47126749113 / 87500000000)$$

$$g = -(643613364349 / 70000000000)$$

$$h = -(832344639197 / 87500000000)$$

$$j = -(3781580520177 / 17500000000)$$

$$d = 600$$

#### Step 2: Define a new function find\_T

This function gives the solution of an equation with one unknown, T:

Find\_T returns the value:  $(d - (b.t.k + g.t + h.k + j)) / (a.t.k + c.k + d.t + f)$ ;

#### Step 3: Define the steps and the Number of solutions

These are the increment by which time and potential vary in their loops.

Herein the chosen steps where:  $\text{step}_t = \text{step}_{Kn} = 5$ . The user could use other steps (not necessarily of the same value). Small steps increase the accuracy as well as the number of solutions.

Define a counter:  $\text{Number\_of\_solutions} = 0$ . This one will keep track of the number of solutions found;

#### **Step 4: Create the first loop**

This loop varies the values of time  $t$  within a given interval. This interval must respect the possible gas nitriding times. The interval chosen herein is [5-120] in hours.

#### **Step 5: Create the second loop**

This loop varies the values of potential  $Kn$  within a given interval. This interval must respect the possible gas nitriding potentials. Since potential is a percentage, the interval chosen herein is [1-99].

#### **Step 6: Solve the equation for T**

The values of time and potential are defined, thanks to the two previous loops. Now the algorithm can easily solve one unknown equation for  $T$  using the function `Find_T`.

In order to find real values of nitriding temperature, the algorithm merely accepts the values of  $T$  that verify the inequality:  $470 < T < 570$ .

After that, the counter increases its value by one:

$\text{Number\_of\_solutions} = \text{Number\_of\_solutions} + 1$ .

It should be noted that the previous algorithm was coded in Python 3.7.6 64-bit implemented in Visual Studio Code 1.45.1.

### **V.3.2 Results and Discussion**

The results of the optimization algorithm were presented after every found solution that verifies the inequality  $470 < T < 570$ , as follows:

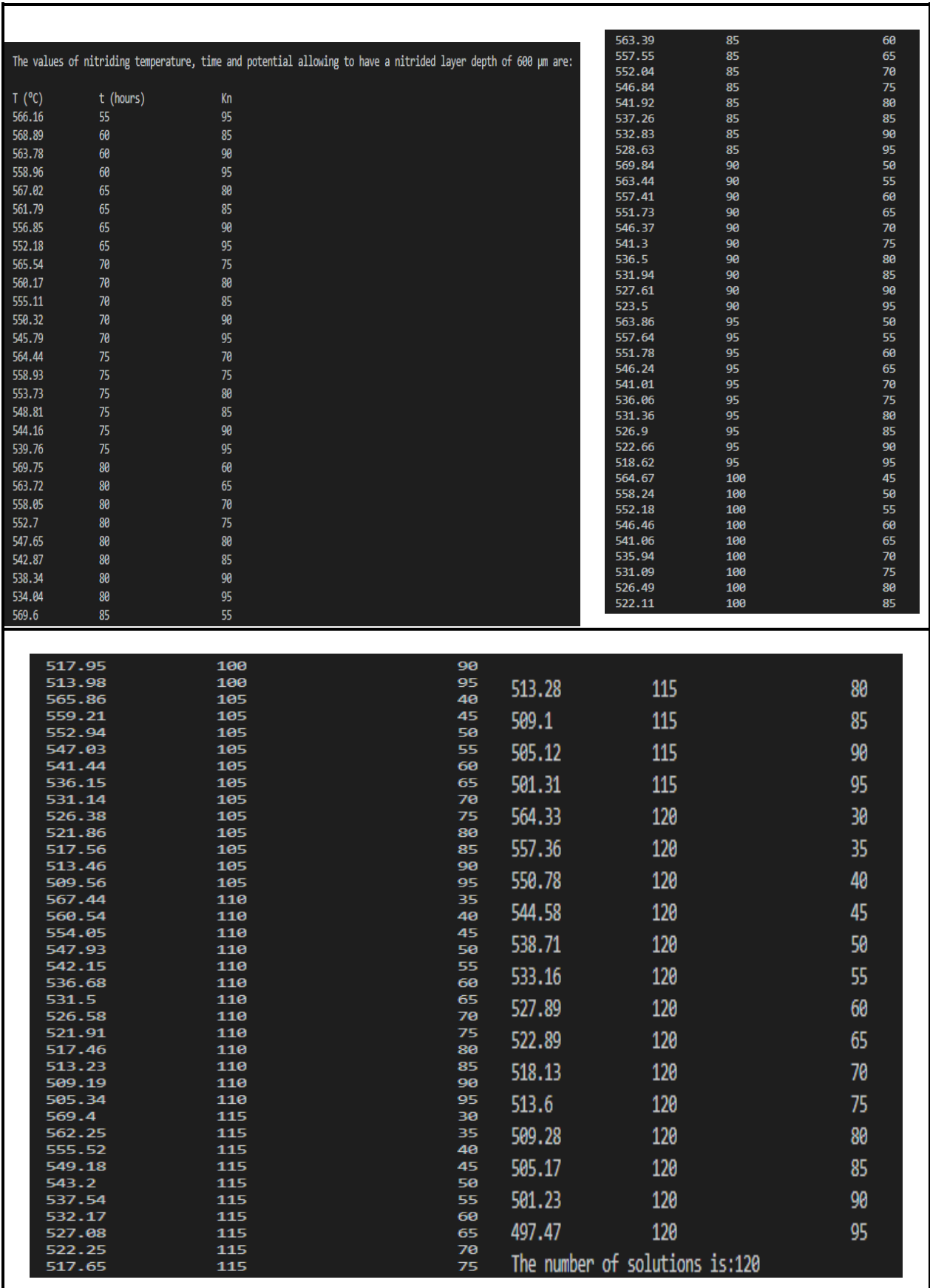


Figure V.1. Output for NL depth of 600µm

Given a number of steps of 5 to the two variables, time and potential, the algorithm found 120 solutions. A smaller or higher number of solutions could have been found with different numbers of steps.

This algorithm has the time as the first loop. This choice means that the first solutions would start with the lowest values of time. Therefore, this algorithm optimizes the response, by means of finding the combinations of parameters allowing to have the best NL depth, from one hand, and on the other hand, it facilitates the process of finding the solutions allowing to find the desired NL depth in the shortest nitriding time.

Minimizing the nitriding time comes with great practical importance for the following reasons:

- Gas nitriding is known to be a long treatment, compared to other types of nitriding and even other surface treatment techniques;
- Higher nitriding times result in higher power consumption, considering that nitriding furnaces consume large amounts of electric power<sup>[23]</sup>;
- Higher nitriding times could harm the nitriding equipment, especially the furnace.

### V.4 Validating the Algorithm

The solutions present values of time, temperature and potential that are within their respective gas nitriding intervals. One way to somewhat validate these results would be by comparing the combinations provided by the algorithm with experimental values of NL depth. As a matter of fact, validating the algorithm is validating the accuracy of the obtained equation. The experimental combination should be found, approximately, in at least one of the combinations provided by the algorithm.

According to the graphs showing the parabolic growth of the NL depth in the work of Mridha (2007), 600 $\mu$ m can be acquired, approximately, with the combination: (T=570, t=60, Kn=80)<sup>[20]</sup>. The closest solution found by the optimization algorithm to this combination is the second one: (T=568.89, t=60, Kn=85), which are in good accordance with the approximation of the aforementioned paper.

In order to further validate the results, a real experimental value of NL depth is tested. Again, in the paper of Mridha (2007), a NL depth of 655.74 was found with the parameters: (T=570, t=72, Kn= 80)<sup>[20]</sup>. By changing the output of the algorithm



( $d=655.74$ ), one of the obtained solutions has given: ( $T=569.32$ ,  $t=70$ ,  $Kn= 85$ ), which is, again, in good accordance with the experimental results obtained by Mridha.

T (°C)	t (hours)	Kn
566.03	65	95
569.32	70	85
564.15	70	90
559.25	70	95
567.92	75	80

Figure V.2 Output in case of NL depth of 655.75µm

Another experimental result found in the paper of Mridha is a NL depth of 553.17 µm reached with the combination ( $T=570$ ,  $t=48$ ,  $Kn=80$ ) and one of the combination found by the algorithm is considerably close to the real experimental combination:

T (°C)	t (hours)	Kn
568.81	45	95
565.88	50	90
561.07	50	95
568.58	55	80
563.35	55	85

Figure V.3 Output in case of NL depth of 533.17µm

The first result shows that this depth could have been found with a shorter nitriding time (45 hours) yet with a higher nitriding potential. This depends on the practical circumstances with regards to the preferability of optimizing any of the parameters.

## V.5 Conclusion

In this chapter, a simple optimization algorithm was developed in Python programming language. The idea was to exploit the equation established in chapter IV giving the nitrided layer depth as function of nitriding temperature, time and potential. The program provided adequate solutions with regards to the practical nitriding parameters. In addition, the algorithm presented the solution in an increasing order of nitriding times, since minimizing this later comes with great practical importance. Finally, the solutions calculated by the algorithm were validated with real experiments, which further confirms the accuracy of the previously obtained equation.

---

# **General Conclusion**

---

## General Conclusion

The work presented in this thesis investigates the application of Design of Experiments in gas nitriding of steels, which has never been attempted in the literature. The DoE was utilized herein as a modeling technique, allowing to determine the factors with the greater influence on the nitrified layer depth and create a mathematical model giving the nitrified layer depth as function of the nitriding temperature, time and potential. Furthermore, this model was exploited in optimization of the nitrified layer depth for a desired value.

It should be mentioned that the steel used in this study was merely an example, as the methods applied in this work are valuable for all nitriding steels. The essential point is the availability of experimental data of gas nitriding of the steel to be studied. These data must be sufficient to establish at least a fractional factorial design.

The main conclusions that can be drawn from this study are the following:

- Full factorial designs are preferable in modeling, considering that they provide higher accuracy than that of fractional ones. Nevertheless, in case of lack of experimental data, fractional factorial designs, such as Taguchi's arrays, can provide acceptable results;
- Nitriding temperature has the greatest influence on the nitrified layer depth, followed by the nitriding potential, and then the nitriding time;
- Using DoE, it is possible to obtain a mathematical polynomial function giving a chosen response as function of its parameters;
- Using the latter function, an experimenter can find the optimum combination of nitriding parameters allowing to acquire the desired nitrified layer depth;
- In the case where very limited combinations of gas nitriding parameters can be applied, it is possible to predict, again, using the latter function, the NL depth that can be reached;
- Most of gas nitriding treatments could be optimized, i.e. performed under lower values of temperature, time and potential, using a DoE model;

### Future work

This work opens a perspective for several future research studies in the domain of modeling the gas nitriding treatment, among which:

- Applying the DoE on other types of nitriding steels;
- Performing experimental works aiming for validating the obtained gas nitriding DoE models;
- Comparing the results of the gas nitriding DoE models with those of other numerical methods, such as Newton and Finite Elements, using Fick's diffusion laws, and with Artificial Intelligence and Machine Learning techniques, such as Artificial Neural Networks (ANN) and Fuzzy Logic (FL);
- Utilizing thermodynamic software, such as Thermocalc, in order to investigate the structures of the formed nitrided layers, which would allow for predicting these structures, using the model's NL function, prior to performing the treatment.

---

# References

---

---

## References

- [1] D. Pye, Practical Nitriding and Ferritic Nitrocarburizing, Materials Park, Ohio: ASM International, 2003.
- [2] RAYANE, Karim, Simulation et Modélisation de la Diffusion Atomique dans les Solides, PhD thesis, University of Amar Telidji, Laghouat, 2016.
- [3] Helmut Mehrer, Diffusion in Solids, Springer Series In Solid-State Sciences 155.
- [4] PYE, David. Practical NITRIDING and Ferritic Nitrocarburizing. Ohio, 2014. 256 p. ASM International.
- [5] Rafael Menezes Nunes et al. Surface Engineering. 1994. 2535 p. ASM Handbook, Volume 5.
- [6] Tohru Arai et al. Heat Treating, ASM Handbook, Volume 4.
- [7] HAMED, Naima, Contribution à l'Etude de la Nitruration des Aciers Faiblement Alliés Au Cr-Mo-V. Relation Microstructure – Propriétés Mécaniques. 144 p. Magister thesis: Metallurgy, Algiers, Ecole Militaire Polytechnique, 2002.
- [8] BENZETTA, Abd El Halim. Nitruration Gazeuse des Aciers Faiblement Alliés Fe-C-Cr, Fe-C-Cr-Al et Fe-C-Cr-V. 125 p. Magister thesis, Mecanique Des Materiaux, Algiers, Ecole Militaire Polytechnique, 2016.
- [9] BENRABIA, Nacer-Eddine, Optimisation des Paramètres de Nitruration. Influence des Eléments d'Addition, Modélisation et Calculs Thermodynamique. 142 p. Magister thesis: Metallurgy, Algiers, Ecole Nationale Polytechnique, 1998.
- [10] M.E. DJEGHLAL, Etude des phénomènes de diffusion, précipitation et évaluations thermodynamiques des phases formées lors de la nitruration des alliages binaires synthétiques et des aciers Cr-Mo-V. PhD thesis, Ecole Nationale Polytechnique, Algiers, 2003.
- [11] D.Ghiglione, C.Leroux, C.Tournier. Pratique des traitements thermo-chimiques, Nitruration, nitrocarburation et dérivés, Techniques de l'Ingénieur, M4 (M1227), 1996.
- [12] Gerster, Härtereier, Hightech by Gerster: Nitruration Gazeuse.
- [13] DJABRI Imad Eddine, Modélisation du Phénomène de Diffusion de l'Azote dans le Fer Pur pour un Traitement de Nitruration, Master thesis, École Militaire Polytechnique, 2016.

- [14] Wang, B., Sun, S., Guo, M., Jin, G., Zhou, Z., & Fu, W. (2015). Study on Pressurized Gas Nitriding Characteristics for Steel 38CrMoAlA. *Surface and Coatings Technology*, 279, 60–64. doi:10.1016/j.surfcoat.2015.08.035.
- [15] L. Ilzarbe et al., *Practical Applications of Design of Experiments in the Field of Engineering: A Bibliographical Review*, Quality And Reliability Engineering International, 2008.
- [16] KARAM, Sandrine, *Application de la Méthodologie des Plans d'Expériences et de l'Analyse de Données à l'Optimisation des Processus de Dépôt*, 243 p. PhD Thesis: Electronique des hautes fréquences et optoélectroniques, Limoges, ECOLE DOCTORALE Science – Technologie – Santé, 2004.
- [17] Howard J. Seltman, *Experimental Design and Analysis*, Carnegie Mellon University, U.S., 2018.
- [18] NIST/SEMATECH e-Handbook of Statistical Methods, <https://doi.org/10.18434/M32189>.
- [19] Živorad R. Lazić, *Design of Experiments in Chemical Engineering*. Weinheim, Germany, 2004. 522 p, ISBN: 3-527-31142-4.
- [20] Mridha, S. (2007). Gas Nitriding of En40B Steel with Highest Growth Rate of the Case and Reduced White Layer Formation. *International Journal of Microstructure and Materials Properties*, 2(1), 54. doi:10.1504/ijmmp.2007.012938.
- [21] John M. Cimbala, *Taguchi Orthogonal Arrays*, Penn State University, September 2014.
- [22] Azouani, Omar, *Traitement Thermo-chimique en Phase Solide des Aciers Utilisant des Poudres (Bore-Silicium) et (Bore- Azote) : Caractérisations des Couches Formées et Cinétique de Diffusion*. Magister thesis, Université Saad Dahlab de Blida, 2013.
- [23] Andreas Gebeshuber, Martin Aigner, Thomas Müller, *A Comparison of Plasma and Gas Nitriding Processes from an Environmental Point of View*, RUBIG GmbH & Co KG, 2020.